Icarus 456 (2026) 117133

Contents lists available at ScienceDirect

Icarus

journal homepage: www.elsevier.com/locate/icarus

Gorgona Island (Colombia) as a terrestrial analog of Syrtis Major (Mars): Evidence from geochemical meta-analyses and compositional figures of merit

D. Tovar [a,b,c,*], M.A. Leal [a,b,g], M.A. de Pablo [b], J. San Martin-Lobos [d], N. Tchegliakova [a,c], F. Vélez [a], A. Molina [b,e], G. Leone [f], J. Sánchez [a,g], A. Torres [h], M.A. Bonilla [g,i], R. Acevedo-Barrios [a,j], G. Cancino-Escalante [k]

[a] Planetary Sciences and Astrobiology Research Group (GCPA), Universidad Nacional de Colombia and Corporación Científica Laguna, 111321 Bogotá, Colombia
[b] Departamento de Geología, Geografía y Medio Ambiente, Universidad de Alcalá, 28805 Alcalá de Henares, Spain
[c] Departamento de Geociencias, Universidad Nacional de Colombia, 111321 Bogotá, Colombia
[d] Technische Universität Bergakademie Freiberg, 09599 Freiberg, Germany
[e] Department of Planetology and Habitability, Centro de Astrobiología (CSIC/INTA), 28850 Torrejón de Ardoz, Spain
[f] Instituto de Investigación en Astronomía y Ciencias Planetarias, Universidad de Atacama, Copiapó, Chile
[g] Departamento de Biología, Facultad de Ciencias, Universidad Nacional de Colombia, 111321 Bogotá, Colombia
[h] Observatorio Astronómico, Instituto Tecnológico Metropolitano de Medellín, 050034 Medellín, Colombia
[i] Biology of Tropical Organisms Research Group, Universidad Nacional de Colombia, 111321 Bogotá, Colombia
[j] Grupo de Estudios Químicos y Biológicos. Dirección de Ciencias Básicas, Cartagena de Indias D.T y C, Universidad Tecnológica de Bolívar, POB 130001, Turbaco, Colombia
[k] Universidad de Pamplona, Pamplona 543058, Norte de Santander, Colombia

ARTICLE INFO

Keywords:
Planetary geochemistry
Terrestrial analogs
Mineralogy
Ultramafic rocks
Figures of merit

ABSTRACT

The identification of terrestrial analogs is a key strategy for advancing our understanding of the geological and geochemical evolution of Mars. This study evaluates the potential of Gorgona Island (Colombian Pacific) as a geochemical analog of Syrtis Major. Gorgona Island hosts a diversity of mafic and ultramafic lithologies, including basalts, gabbros, picrites, dunites, wehrlites, and also komatiites, which are the youngest reported on Earth. To assess the degree of compositional similarity, a meta-analysis of previously published data was conducted, comparing geochemical information from Gorgona Island with that derived from orbital instruments on Mars (TES, GRS, OMEGA, and CRISM) and from SNC meteorites. The analysis focused on classical discriminant ratios (Al_2O_3/TiO_2) and Compositional Figures of Merit (FOMc), applied both to individual datasets and to averaged values weighted by the areal proportion of lithologies on Gorgona Island. The results show that enriched and depleted basalts, along with Spinifex-Textured komatiites (containing <18% MgO), exhibit a high degree of geochemical similarity with Syrtis Major (FOMc >0.87), whereas dunites and wehrlites consistently display low values. The positive slope of the Al_2O_3/TiO_2 ratio observed in both Gorgona and Mars is characteristic of MORB-type oceanic crust, reinforcing the link between Terrestrial MORB/OIB and Martian Basalts described by previous studies. These findings highlight Gorgona Island as a robust terrestrial analog of Syrtis Major, providing a natural laboratory for investigating magmatic processes relevant to Mars. Furthermore, this work outlines future directions, including the acquisition of new high-resolution geochemical data from Gorgona Island and the integration of recent in situ data from Mars, with the aim of refining comparative models of planetary magmatism.

* Corresponding author at: Planetary Sciences and Astrobiology Research Group (GCPA), Universidad Nacional de Colombia and Corporación Científica Laguna, 111321 Bogotá, Colombia.
E-mail address: david.tovar@edu.uah.es (D. Tovar).

https://doi.org/10.1016/j.icarus.2026.117133
Received 21 November 2025; Received in revised form 4 April 2026; Accepted 27 April 2026
Available online 28 April 2026

1. Introduction

1.1. Mafic minerals in the Syrtis major region

The Martian crust exhibits a compositional affinity with the terrestrial oceanic crust, dominated by extrusive igneous rocks, primarily pyroxene-rich basalts (Christensen et al., 2003; Bibring, 2005; Chevrier and Mathé, 2007). This similarity indicates comparable magmatic processes occurring in distinct tectonic contexts, with limited crustal differentiation on Mars. In Syrtis Major, compositions dominated by basalts with mineralogy akin to terrestrial basalts have been identified, including the presence of olivine at the NE sector of Syrtis Major (Black and Manga, 2016; Bandfield, 2002; Ehlmann et al., 2008; Clenet et al., 2013; McSween Jr, 2015; Salvatore et al., 2018; Liu et al., 2022). Additional findings of olivine and spectroscopical traces of Mg carbonates in the eastern portion of Nili Fossae further underscore the importance of this sector for reconstructing the thermal and volcanic history of Mars from the Early Noachian to the present (Ehlmann, 2008; Brown et al., 2020).

Previous studies have consistently indicated that Syrtis Major is dominated by mafic rocks, with geochemical ranges suggesting ultramafic affinities (Bandfield, 2002; McSween, 2015; Liu et al., 2022). Orbital datasets (TES, CRISM, OMEGA) and SNC meteorites reveal compositions characterized by elevated FeO_t (14–18 wt%), moderate to high MgO (6–18 wt%), and low TiO_2 (<1 wt%), defining a pattern typical of basalts and pyroxenites, with compositions in some cases approaching primitive lithologies similar to depleted komatiites (Demchuk, 2021; Duktig, 2023). This interpretation is reinforced by spectral analyses identifying olivine and clinopyroxene as dominant phases and, to a lesser extent, calcic plagioclase (Mustard et al., 1993; Reyes and Christensen, 1994; Liu et al., 2022), a mineralogical assemblage consistent with high-temperature, low-viscosity magmas comparable to those generated on the early Earth (McGetchin and Smith, 1978; Stolper and McSween Jr, 1979).

The possible existence of ultramafic rocks on Mars, particularly komatiites, has been the subject of debate for decades. Based on data from the Imaging Spectrometer for Mars (ISM) onboard the Phobos 2 mission, Mustard et al. (1993) concluded that Syrtis Major was dominated by basalts rich in calcic pyroxene, with little evidence of olivine and variability explained by dust and altered soils. However, Reyes and Christensen (1994) re-analyzed the same dataset and proposed the presence of lavas with komatiitic affinity by comparing them with (1) terrestrial komatiites, (2) Apollo 12 lunar basalts, and (3) SNC meteorites. Their results suggest komatiitic basalts formed at high temperatures and low viscosity (Rampey and Harvey, 2012).

Recent studies have revitalized this discussion. Liu et al. (2022), using in situ data from the Perseverance rover in Jezero Crater (PIXL, SuperCam, SHERLOC, and Mastcam-Z instruments), described olivine-rich lithologies (Fo ~50–65) that could originate from fractional crystallization processes of mafic and ultramafic magmas, within magma chambers or at the base of low-viscosity lava flows. Taken together, studies in Syrtis Major reveal three common points: 1) the predominance of mafic materials (pyroxenes and olivines), 2) the use of spectroscopic techniques for mineralogical characterization, and 3) the association with textures and minerals typical of high-temperature, low-viscosity magmas, comparable to komatiites (McSween, 2015).

This study compiles relevant geochemical information from the Syrtis Major region, located at quadrangle MC-13 (Fig. 1), including: (1) data from remote sensing instruments aboard orbiters, and (2) analyses of SNC-type meteorites believed to originate from this area. Therefore, it was initially selected as a primary site for detailed study and for comparison with similar terrestrial lithologies (e.g., Gorgona Island). It is important to note that other regions on Mars may also contain similar lithologies; however, the extensive amount of analyzed and published data available for Syrtis Major was a key criterion considered by the research team for this study.

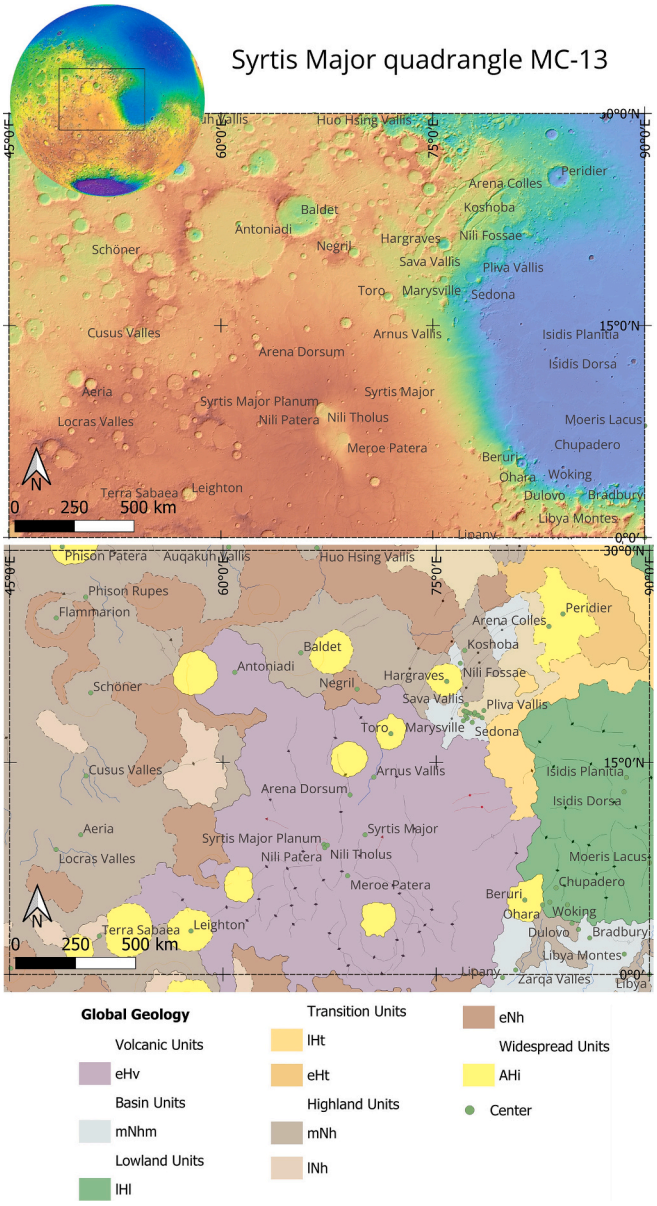

Fig. 1. Syrtis Major location (a) and geological features (b) [Single column figure].

1.2. Geological context of Gorgona Island

Gorgona Island, located in the Colombian Pacific about 30 km off the continental coast, consists of the main island and Gorgonilla (Fig. 2), both sharing similar compositions (Kerr, 2005). This locality hosts a diverse suite of lithologies: basalts, gabbros, dunites, picrites, wehrlites, and, exceptionally, komatiites (Echeverría, 1980; Serrano et al., 2011). The latter, with a Cretaceous age (~90 Ma), are considered the youngest on the planet and the only ones formed during the Phanerozoic, in contrast to the typical Archean and Proterozoic provinces such as Barberton, Abitibi, or Fennoscandia (Arndt et al., 1977, 1997Kerr, 2005; Arndt et al., 2008; Serrano et al., 2011). Their study has generated intense debates regarding origin and geodynamic context, including the hypothesis of a high-temperature mantle plume (Storey et al., 1991), a heterogeneous mantle with enriched and depleted components (Arndt et al., 1997; Kerr, 2005), and their relation to the evolution of the Caribbean Large Igneous Province (henceforth CLIP) (Kerr et al., 1996a; Shimizu et al., 2009). Subsequent research has complemented this view with tectonic analyses and radiometric datings that link Gorgona Island

Fig. 2. Location of Gorgona Island in Colombia (red triangle; image source: ESRI Satellite World Imagery). [DOUBLE COLUMN FIGURE]. (For interpretation of the references to colour in this figure legend, the reader is referred to the web version of this article.)

to processes of deep partial melting and plume–oceanic lithosphere interaction (Echeverría and Aitken, 1986; Révillon et al., 2002; Serrano et al., 2011; Gurenko et al., 2016). Additional studies show that the CLIP originated as a result of a complex interaction between a hot mantle plume (similar to the Galápagos plume) and the Mesozoic oceanic lithosphere, within an intra-oceanic setting whose magmatic activity is estimated to have lasted approximately 140–170 Ma. This process led to large-scale melting of the upper mantle, generating mafic and ultramafic rocks with geochemical characteristics such as low concentrations of incompatible elements and trace element signatures indicative of formation under high-temperature conditions (Riel et al., 2023).

1.3. Geochemistry of mafic and ultramafic rocks in Gorgona Island and Syrtis Major

The komatiites of Gorgona exhibit characteristic spinifex textures and are divided into two geochemical groups: one enriched in light rare Earth elements (LREE) (La/SmN > 1) and another depleted (La/SmN < 1), reflecting mantle heterogeneity (Kerr et al., 1996b; Arndt et al., 2008). Younger examples (~64 Ma), with low K and high Mg, suggest high degrees of partial melting associated with a slab window context rather than a mantle plume (Grove and Parman, 2004). Melt inclusions in olivine indicate crystallization temperatures of 1330–1340 °C under hydrous conditions, consistent with a heterogeneous and hydrated mantle (Kamenetsky et al., 2010; Serrano et al., 2011). It is important to note that in this study, Gorgona Island Komatiites with <18% MgO (geochemically classified as picrites by the IUGS; Lustrino et al., 2020), refer to Spinifex-textured Komatiites suggested by Kerr and Arndt (2001) (Gill, 2011).

Basalts constitute the most abundant extrusive unit and display variations ranging from picritic to tholeiitic basalts, with MgO contents between 6 and 10% and, in some cases, enrichment in FeO_t. They exhibit subophitic and porphyritic textures and are interlayered with komatiitic flows, reflecting a complex eruptive evolution and the coexistence of magmas of different compositions (Kerr et al., 1996a; Serrano et al., 2011). Geochemically, they also display enriched and depleted LREE groups, with Ar—Ar ages between ~85.7 and 69.6 Ma, indicating a progressive increase in the degree of partial melting (Kerr, 2005).

Although komatiites and basalts on Gorgona Island constitute the most representative lithological units of this volcanic island, also gabbros, picrites, dunites, and wehrlites, provides a natural laboratory for exploring magmatic processes linked to mantle evolution and Large Igneous Provinces (LIP's). This combination makes it an appropriate setting for applying geochemical analyses and Figures of Merit to evaluate its potential as a compositional analog of the Syrtis Major region on Mars.

Dilemma regarding the presence of komatiites in the Syrtis Major region require additional data sets or analyses to determine mineralogical and geochemical similarities. The observation of spinifex texture, typical of these rocks, would constitute one of the key lines of evidence for their identification; however, recognizing this texture is unfeasible with the spectroscopic techniques currently available. Nesbitt et al. (1979) emphasized that spinifex texture is a primary indicator of ultramafic magmas generated at very high temperatures, but in cases

where it is not preserved, discrimination must rely on robust geochemical parameters, such as the Al_2O_3/ TiO_2 ratio, which allows ultramafic rocks to be distinguished from typical basalts (Nesbitt et al., 1979; Waterton and Arndt, 2023; Mendes et al., 2025).

In this context, this study focuses on a meta-analysis of existing geochemical data from the literature in order to establish the geochemical and mineralogical nature of the materials in the Syrtis Major region, comparing them with data from a terrestrial region containing materials of a similar nature (i.e., Gorgona Island). Therefore, we use a methodology based on geochemical meta-analysis and Figures of Merit (FOM), specifically of the compositional type. Figures of merit constitute quantitative metrics designed to evaluate compositional similarity between materials through the comparison of normalized geochemical vectors, thereby enabling robust assessments of affinities between terrestrial analogs and planetary datasets. For this purpose, we employ published data from the Thermal Emission Spectrometer (TES), Gamma Ray Spectrometer (GRS), and visible–infrared spectroscopy (OMEGA, CRISM) reported in the works of Demchuk (2021), Duktig (2023), Baratoux et al. (2011), Taylor et al. (2010), Poulet et al. (2009), Nair and Mathew (2017) and Rani et al. (2022). These also emphasize the mineralogical composition of the Syrtis Major region, together with mineralogical information from SNC meteorites (Meyer, 2012a, 2012b, 2012c).

FOM are supported by meta-analysis data, fundamental for synthesizing robust evidence and guiding proper interpretation based on accumulated data (Trikalinos et al., 2008). This statistical technique dates back to the 17th century, when it was first applied in the field of astronomy, and was later formalized and mathematically refined by Karl Pearson in the early 20th century and by Gene Glass, who coined the term meta-analysis in the 1970's (Egger et al., 2002). The main objective of implementing this technique is to combine results obtained from independent but comparable studies in order to achieve a more precise estimation of a particular phenomenon. Although meta-analysis has been widely implemented in fields such as medicine, psychology, and the social sciences, its application has expanded beyond these areas, becoming a key technique for interdisciplinary and multidisciplinary research (Sutton and Higgins, 2008). Meta-analysis approach, systematically integrates previously published data on the mineralogical and lithological composition of Gorgona Island and Syrtis Major, with the aim of assessing the degree of compositional similarity between the lithologies present in both localities. The methodology provides relevant data for: 1) elaboration of Al_2O_3/TiO_2 diagram along with TAS diagrams (including data from analog terrains in Hawai'i), Jensen diagram (for the classification of high-MgO rocks), and Al_2O_3/TiO_2 vs. MgO plots (for classification and comparison with MORB); and 2) the calculation of compositional Figures of Merit (FOMc), following the definition established in ISO 10788:2014 and outlined by Rickman et al. (2007), and implemented to the characterization of asteroid (e.g. Metzger et al., 2019), Martian (e.g., Fackrell et al., 2021; San Martin et al., 2025), and lunar simulants (e.g. Schrader et al., 2010). This methodological design allows for the evaluation of compositional compatibility through normalized metrics and specific elemental ratios, thereby increasing the robustness of the analysis and providing key evidence of geochemical similarities between lithological units on Gorgona Island as well as the Syrtis Major region on Mars.

2. Materials and methods

To evaluate the potential of Gorgona Island as an analog of Mars, a methodology was designed based on the integration of geochemical data from multiple previously conducted studies. This approach combines the use of geochemical meta-analysis (Mikolajewicz and Komarova, 2019), which allows for the systematic synthesis and comparison of results dispersed throughout the literature, with the application of compositional Figures of Merit (FOMc) and discriminant geochemical parameters. The methodological framework is organized into three stages: 1) compilation and classification of published data on Gorgona Island, Syrtis Major, and Martian meteorites; 2) normalization and homogenization of these datasets to ensure comparability; and 3) application of quantitative similarity metrics, including oxide ratios and compositional Figures of Merit (FOMc), in order to objectively establish the degree of compatibility between both sets of lithologies. The methodology is also shown as a flow diagram (Fig. 5.).

2.1. Data selection

This study compiled the data available from previously published literature. For Gorgona Island, geochemical data were obtained from eleven classical and recent studies that employed electron probe microanalysis (EPMA) and X-ray fluorescence (XRF) (Echeverría, 1980; Dietrich et al., 1981; Aitken and Echeverría, 1984; Echeverria, 1986; Brügmann et al., 1987; Kerr et al., 1996a, 1996b; Arndt et al., 1997; Révillon et al., 2000; Kerr, 2005; Serrano et al., 2011).

Geochemical composition of mafic rocks on the Martian surface, corresponding to Quadrangle 13 in the Syrtis Major region, was obtained through an analysis of two main datasets: 1) compositions of Martian SNC meteorites (shergottites, nakhlites, and chassignites) (Vickery and Melosh, 1987) and 2) geochemical estimates of the Syrtis Major region derived from orbital remote-sensing techniques.),

2.1.1. SNC meteorite geochemical data

These include Shergotiite meteorites that are compositionally and spectrally representative to Syrtis Major rock compositions (Mustard et al., 1993; Ody et al., 2015; Reyes and Christensen, 1993, 1994), namely, basaltic shergottites Los Angeles, Shergotty and QUE 94201 (Ody et al., 2015). Some studies link Syrtis Major as a possible source, however this implies an older formation age (Bouvier et al., 2009; Ody et al., 2015; Udry et al., 2020). Conversely, some consider these sourced from younger amazonian terrains (Cohen et al., 2023; McSween et al., 2023; Nyquist et al., 2001), which would associate it with Tharsis, Amazonia and or Elysium volcanic provinces (McSween, 2002; Nyquist et al., 2001) and their impact craters (Hamilton et al., 2020; Herd et al., 2017; Lagain et al., 2021; Tornabene et al., 2006). Nakhla and Chassigny group meteorites have also been compositionally linked to NE Syrtis Major and Nili Fossae region, and have also been considered as a potential source location (Hamilton et al., 2003; Harvey and Hamilton, 2005a, 2005b; Kereszturi and Chatzitheodoridis, 2016; Ody et al., 2015). However, inconsistencies regarding their impact crater and formation age have also been pointed out (Lang et al., 2009) (Mustard et al., 1993, 1997; Hamilton et al., 2003; Ody et al., 2015; Werner et al., 2014).

2.1.2. Remote sensing derived geochemical data

This includes major and minor oxide data from Gamma-ray spectroscopy (Mars Odyssey GRS) (Baratoux et al., 2011; Rani et al., 2022; Taylor et al., 2010), Its bulk geochemistry using the Mass balance calculation method by Baratoux et al. (2014), and bulk geochemical compositions derived from modal mineralogy obtained from spectral deconvolution of Mars Global Surveyor's Thermal Emission Spectrometer (TES) (Demchuk, 2021; Duktig, 2023), and Odyssey's VIR mineralogical Mapping spectrometer (OMEGA) data (Poulet et al., 2009).

GRS data only provides elemental abundance of Si, Fe, Al, K, Th along with a few volatile elements (H, S and Cl) (Gary-Bicas et al., 2026; Hood et al., 2016; Rani et al., 2022) (which can be converted to oxide abundance assuming Iron is in the Fe^{+2} oxide state; Baratoux et al., 2014). In order to determine Na_2O, TiO_2, P_2O_5, MnO and MgO abundances, Baratoux et al. (2014) used Mass balance calculations. These consists of using minor oxide ratios derived from Basaltic shergottite compositions, to calculate the missing oxides using GRS data as reference (based mostly K_2O GRS data). MgO is calculated as the difference of the sum total oxide (100 wt%) (Baratoux et al., 2014), assuming all other oxide values are constrained (Hughes et al., 2024). Hughes et al.

(2024) further refines this method by providing oxide ratios derived from in-situ analysis (Gale crater, Gusev crater, Meridiani planum and average RAT abraded Pristine Igneous Rocks) and Regression method using Mg/Si and Ca/Si ratios of Martian meteorites to compute MgO abundances from GRS CaO and SiO_2 data.

In this study, both compositions are used to calculate GRS derived Bulk geochemical composition of the Syrtis Region, using Hughes et al. (2024) Pristine Igneous Rocks ratios and Taylor et al. (2010) and Rani et al. (2022) Syrtis Major GRS data (Table 1 and Supplementary Material 1).

TIR Spectral deconvolution has been used in multiple studies to characterize the composition of the Martian surface on a global (Bandfield, 2002; Christensen et al., 2000b; Hamilton et al., 2001; Greenough and Ya'acoby, 2013) and regional scale (Demchuk, 2021; Duktig, 2023; Dunn et al., 2007; Hood et al., 2016; Hughes et al., 2024; Poulet et al., 2009; Zalewska et al., 2018). This method consists of separating or deconvolving the thermal Infrared spectra of surface rocks into the summed emitted spectra of their constituent minerals (Hamilton and Christensen, 2000), through the use of a linear least squares deconvolution technique (Ramsey and Christensen, 1998) and selection of known end-member minerals from mineral spectral libraries (e.g. Christensen et al., 2000a). This allows to derive the volumetric percentages of constituent minerals (model mineralogy), from which the bulk geochemical composition of the analyzed surface can be calculated (Wyatt et al., 2001).

Regarding the Syrtis Major region, spectral deconvolution derived bulk geochemical compositions of central-South Syrtis Major lavas (65°-69°E, 1.5°-12°N), were determined by Poulet et al. (2009) and Syrtis Major Planum and Antoniadi Crater (50–85°E,~5°S-25°N) were estimated by Demchuk (2021) and Duktig (2023). The latter studies define the composition of multiple thermophysical units, which were delimited and interpreted as distinct lava flows by thermal contrasts in nighttime brightness temperatures from THEMIS thermal infrared images, surface physical properties (e.g. elevation and surface texture) and morphological features (e.g. lava lobes) (Demchuk, 2021). Geochemical compositions of each Thermophysical unit derives from the deconvolution of compiled (average) MGS-TES spectral data taken from multiple 3 × 3 km to 3 × 9 km areas of measurement within the unit (Demchuk, 2021). Location of TES "stamps" by Duktig (2023), and selected minerals for spectral deconvolution of Demchuk (2021), Duktig (2023) and other studies are available in the Supplementary Material 2).

Both meteorite and orbital remote sensing bulk geochemical composition datasets were organized and integrated into a unified database focused on major and minor oxides (SiO_2, TiO_2, Al_2O_3, FeO, MgO, CaO, Na_2O, K_2O, P_2O_5, MnO), enabling direct comparisons (FOM analysis). Moreover, Thermophysical unit compositions were organized and categorized according to chronological and stratigraphic relations defined by Fawdon (2016) (Fig. 3), which contains units ranging from the Late Noachian, Early and Late Hesperian and Amazonian (Fawdon, 2016; Platz et al., 2014). Although Demchuk's (2021) and Duktig's (2023) Thermophysical units can encompass multiple stratigraphic units, the absolute ages provided by Fawdon (2016) allows to further constrain these units chronologically and integrate compositional and stratigraphic data. From this, the thermophysical units can be categorized from late Noachian (>3.95 Ga), late Noachian-Early Hesperian (3.95–3.48 ± 0.01 Ga), Early Hesperian (3.60–3.48 ± 0.01 Ga), Early-Late Hesperian (3.60–3.34 ± 0.04 Ga), Late Hesperian (3.36 ± 0.02–3.23 Ga) and Amazonian (2.35 ± 0.25–1.06 ± 0.19 Ga) (a summary of Fawdon's (2026) age determination method and additional detailed information is available in Supplementary Material 2).

2.2. Data normalization and organization

To ensure comparability between datasets obtained through different analytical methods (EPMA, XRF, orbital spectral estimates) and originating from distinct geological contexts (Gorgona Island vs. Syrtis Major and SNC meteorites), a normalization and organization process was implemented at four levels: (1) data cleaning and quality control, (2) compositional homogenization, (3) structuration by lithologies, and (4) areal weighting of the geological units used for calculating one of the FOMc methods.

2.2.1. Data cleaning and quality control

First, all databases were unified into a master table (Supplementary Material 1) with mandatory minimum metadata per analysis: sample identifier, provenance (Gorgona / Syrtis / SNC), geological unit (when applicable), assigned lithology (basalt, komatiite, gabbro, picrite, dunite, and wehrlite), and their source references. When values were

Table 1
Summary of the data used for the meta-analysis and compositional Figures of Merit of Syrtis Major (Mars) and Gorgona Island (Earth).

Planet	Data type	Number of data	Martian Ages						Reference
			Late Noachian	Late Noachian - Early Hesperian	Early Hesperian	Late Hesperian	Early Hesperian - Late Hesperian	Amazonian	
Mars	TES	4	X	–	–	–	–	–	Fawdon (2016), Demchuck (2021), Duktig (2023)
		8	–	X	–	–	–	–	
		8	–	–	X	–	–	–	
		10	–	–	–	X	–	–	
		15	–	–	–	–	X	–	
		2	–	–	–	–	–	X	
	Meteorite	3	–	–	–	–	–	–	Lodders (1998); Rubin et al. (2000); Meyer (2012); Ody et al., 2015
	Syrtis Major TES	1	–	–	–	–	–	–	Poulet et al. (2009)
	Syrtis MajorGRS	4	–	–	–	–	–	–	Taylor et al. (2010); Rani et al. (2022)
Earth	Basalt D	16	–	–	–	–	–	–	Echeverria, 1980; Dietrich et al., 1981; Aitken and Echeverría, 1984; Brügmann et al., 1987; Arndt et al., 1997; Kerr et al., 1996a; Kerr et al., 1996b; Révillon et al. (2000); Kerr, 2005; Serrano et al. (2011)
	Basalt E	21	–	–	–	–	–	–	
	Komatiite (<18)	31	–	–	–	–	–	–	
	Komatiite (>18)	28	–	–	–	–	–	–	
	Gabbro (Gb)	28	–	–	–	–	–	–	
	Picrite	23	–	–	–	–	–	–	
	Wehrlite	3	–	–	–	–	–	–	
	Dunite	4	–	–	–	–	–	–	

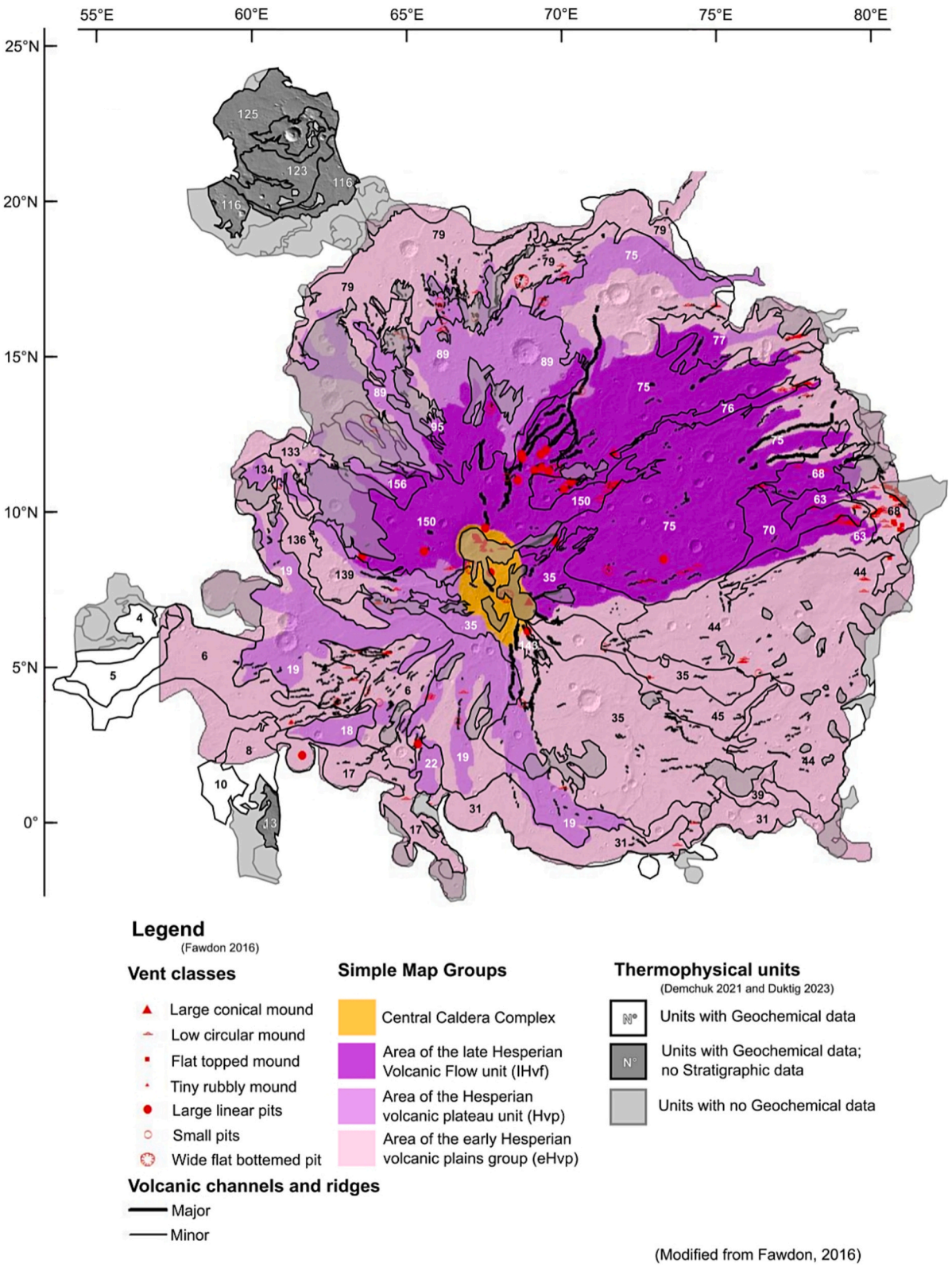

Fig. 3. Map modified from Fawdon (2016) of Syrtis Major planum Shield volcano with simplified stratigraphic units (IHvf, Hvp, eHvp) and overlayed thermophysical units of Demchuck (2021) and Duktig (2023). Due to the low count of TES data "stamps" of, most Amazonian units (Amazonian/Hesperian dark plain units), consisting of small, thin lava flows mostly found in the SW and N of Syrtis Major planum, these are compositionally not represented within the larger thermophysical units (except unit 76, which coincides with Fawdon's (2016) delimited Amazonian volcanic field units). Antoniadi crater units are considered as early-late Hesperian age (Greeley and Guest, 1987; Hiesinger and Head III, 2004), while unit 13 is considered of Late Noachian age (Demchuk, 2021; Duktig, 2023). Summarized data has been compiled in Table 1. (All data analyzed by authors can be found in Supplementary Material 1).

reported below the detection limit, half of the reported limit was assigned; if the limit was not provided, the component was marked as absent to exclude it from calculations that explicitly require it.

2.2.2. Compositional homogenizations

To ensure comparability across datasets, all compositions were normalized lost of ignition (LOI-free) and to 100% by dividing each major oxide by the sum of major oxides and multiplying by 100, as shown in eq. (1). In symbols, for each sample and each oxide *i*:

$$Xi = \frac{\Sigma Xj}{\Sigma Xj - \Sigma X_{LOI}} \times \frac{100}{\Sigma Xj} \quad (1)$$

where *Xi* is the content in wt% (LOI-free), and the summation runs over the available major oxides. To maintain comparability across all metrics, a common compositional vector of ten major oxides (Table 2) is used.

It is important to note that the geochemical datasets from Demchuk (2021) and Duktig (2023) show compositional differences, such as overestimation of TiO_2 (3–10.8 wt%) and K_2O (~1.0–3.5 wt%) (Duktig, 2023), and underestimation of the total oxides (~90%) (Demchuk, 2021). The former may be attributed to the unique selection by Duktig (2023) of ilmenite and Sanidine minerals for the spectral libraries used for spectral deconvolution (Supplementary Material 1). Both datasets also differ from typical Martian compositions. Apart from the overestimated K_2O, TiO_2 (highest known values are from Gusev crater Wishstone and Watchtower class rocks; <3 wt%; Clark et al., 2006), and the lack of P_2O_5 values (Duktig, 2023), these present underestimated FeO values, well below the concentrations typically reported for Mars in-situ and GRS compositions (~10 wt% vs. 15–20 wt%) (Christensen et al., 2003; McSween Jr et al., 2009; McSween 2015; Taylor et al., 2010).

SiO_2 values are also overestimated, which in this case may be affected by the low concentration of FeO in the oxide proportion, but is generally attributed to partial weathering of rock surfaces or the presence of amorphous silica (McSween and McLennan, 2014; Salvatore et al., 2010). For these reasons, along with its comparatively deeper sampling depth (few tens of cm, compared to TES upper 100 μm; Wyatt and McSween, 2007), GRS compositions are considered more accurate than TIR derived compositions (McSween et al., 2023; McSween and McLennan, 2014) (Table 2; Fig. 4 and Supplementary Material 1).

Therefore, TES derived Geochemical FeO and K_2O data was adjusted to fit GRS FeO (20.5–17.5 wt%) and K_2O (0.35–0.39 wt%) geochemical reference data of Syrtis Major provided by Baratoux et al. (2011), Taylor et al. (2010) and Rani et al. (2022) (Supplementary Material 1).

The calculations used for adjusting Demchuk (2021) and Duktig (2023) data sets to the GRS FeO and K_2O reference values and subsequent adjustment of the oxide proportions derive from San Martin et al. (2025) reduction factor calculation:

$$RF = \frac{\Sigma X - |Xi - Xi_{Ref}|}{\Sigma X}, Xi_{Ref} = \{FeOt_{GRS}, TiO_{2\ MET}, P_2O_{5\ MET}, K_2O_{GRS}), \Sigma X = 100 \quad (2)$$

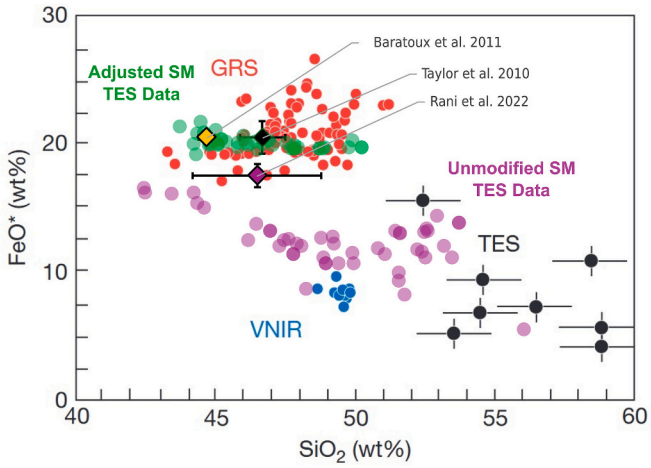

Fig. 4. Comparison of FeO and SiO_2 wt% abundances derived from VNIR (Poulet et al., 2009), TES S1 and S2 surface compositions from (Bandfield, 2002; McSween et al., 2003b), GRS Global Orbital datasets (McSween and McLennan, 2014), Syrtis Major GRS (with root means square uncertainty (±σ); Baratoux et al., 2011; Rani et al., 2022; Taylor et al., 2010), and Syrtis Major (SM) FeO and K_2O adjusted (this study), and unmodified TES compositions (Demchuk, 2021; Duktig, 2023). It's important to note that part of the unmodified SiO_2 values can also be proportionally reduced by the overestimation of TiO_2 (<10 wt%) values of Duktig's (2023) data. Modified from McSween et al. (2023) and McSween and McLennan (2014).

$$adjustment\ Xi \rightarrow Xi_{Ref} \{Xi_{GRS}\ \ Xi \times RF + |Xi - Xi_{Ref}|\ Xi_{MET}\ \ TiO_2 = 0.7278 \times Na_2O; P_2O_5 = 0.8688 \times TiO_2\ \} \quad (3)$$

$$Adjustment\ of\ oxide\ proportion \begin{cases} Xi < Xi_{Ref}\ \ X_{ox} \times RF\ Xi \\ > Xi_{Ref}\ \ X_{ox} \times \frac{1}{RF} \end{cases}, \ \Sigma X_{ox} + Xi_{Ref} = 100 \quad (4)$$

Eqs. 2,3 and 4 are calculated for each time a value is adjusted to the reference, were X_{ox} are all oxides except the adjusted value *Xi*. Considering the clear overestimation of TiO_2 and the lack of P_2O_5 values, Baratoux's et al. (2014) method of using Shergottite meteorite oxide ratios to calculate minor element abundances from GRS major oxides, was used to convert and replace. Duktig's (2023) elevated TiO_2 compositions and provide P_2O_5 data to complete oxide bulk compositions. Reduction factor calculations were also used to adjust the oxide proportions following this modification.

To verify the validity of these modifications, the adjusted Syrtis Major TES compositions were compared to GRS oxides SiO_2, Al_2O_3, CaO (Baratoux et al., 2011; Taylor et al., 2010; Rani et al. (2022) and MgO derived from Baratoux et al. (2014) (~10–7.3 MgO wt%) and Hughes

Table 2
Mean values of major oxides results for Martian units (Noachian, Hesperian, Amazonian and Syrtis Major) and SNC meteorites. Values in bold fall within Syrtis Major GRS and MgO map compositional range (no reference data for TiO_2, MnO, P_2O_5 and Na_2O).

Analogy analysis (Average)	SiO_2	TiO_2	Al_2O_3	FeO	MgO	MnO	CaO	K_2O	P_2O_5	Na_2O
Late Noachian (LN)	48.23	0.61	10.2	19.7	8.31	0.14	9.84	0.37	0.45	2.11
Late Noachian - Early Hesperian (LN-EH)	47.22	0.72	10.46	19.97	8.12	0.15	10.25	0.37	0.62	1.9
Early Hesperian (EH)	45.73	0.84	10.24	20.28	8.91	0.18	10.83	0.37	0.72	1.66
Late Hesperian (LH)	46.32	0.77	9.79	19.89	9.06	0.17	10.98	0.37	0.66	1.75
Early Hesperian - Late Hesperian (EH-LH)	46.12	0.89	10.07	20.10	8.41	0.16	11.10	0.38	0.84	1.62
Amazonian	46.77	0.62	9.2	20.28	9.67	0.15	10.53	0.37	0.48	1.71
Meteorites	47.68	0.61	12.77	15.50	9.26	0.25	10.54	0.29	0.74	2.36
Syrtis Major - TES	49.85	0.2	15.12	8.51	9.51	0.1	14.71	0.1	0	1.9
Syrtis Major - GRS	44.11	0.77	10.98	17.96	13.55	0.31	7.98	0.36	1.05	2.45

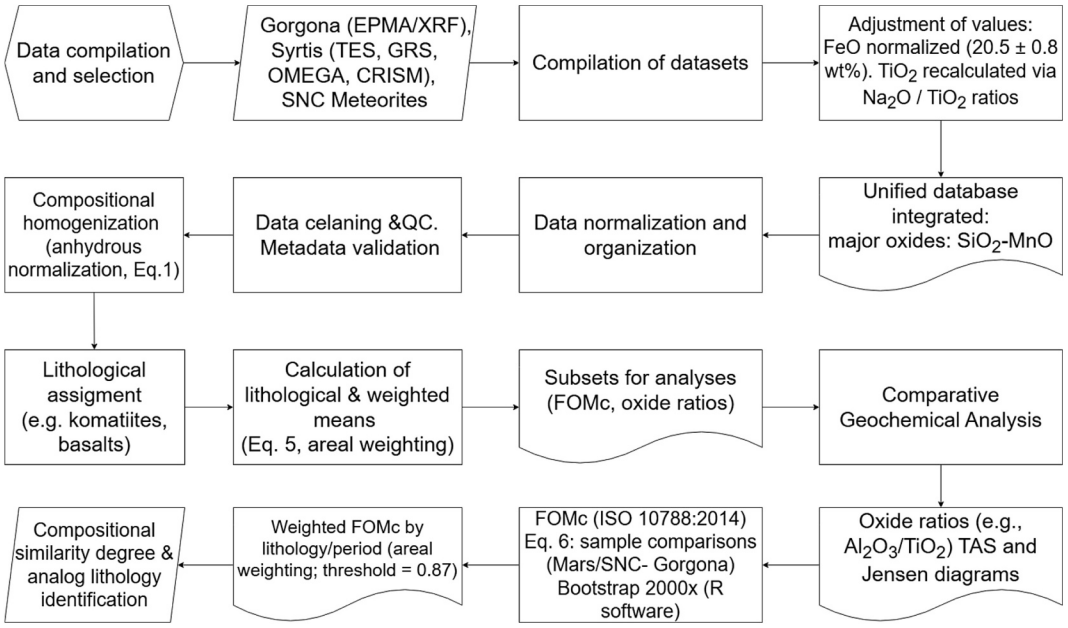

Fig. 5. Flow diagram summarizing the methodology used in this research. Preparation (hexagon), data (inclined rectangle), process (rectangle), documents (rectangle with curved base). [DOUBLE COLUMN IMAGE].

et al. (2024) (11.4–14.69 MgO wt%; Mass Balance method, 18.9–9.37 wt% regression method), which were not directly modified but reduced as consequence of the oxide proportion adjustment (of which, SiO_2 is particularly susceptible; San Martin, 2025). Values outside of the reported root means square uncertainty ($\pm\sigma$) of GRS major oxides may indicate compositional deviations from the true value (GRS absolute abundances) (Supplementary Material 1). The results show that 21 and 12 compositions of the total 44 TES derive compositions, have minor overestimation of CaO and underestimation of Al_2O_3, respectively ($<$ $\pm$2 Δwt% regarding Taylor et al., 2010 and Rani et al., 2022 uncertainty upper and lower limit). However, these are comparatively less than the variation of Poulet et al. (2009) VNIR derived data (+5.62 Δwt%, +3.61 Δwt%, respectively). It is also important to note GRS data represents the average composition of the Syrtis Major province/region; therefore, minor geochemical variability of its constituent units is plausible.

2.2.3. Lithological assignment and organization by geological units

The Gorgona samples were classified into different lithologies (komatiites, basalts, gabbros, picrites, dunites, and wehrlites) and, when the source allowed, into sub-lithologies (e.g., komatiites with MgO $>$ 18 wt% vs. MgO $<$ 18 wt%; basalts enriched/depleted in LREE). Each analysis was linked to its geological unit according to published cartographies; when the sources considered the combined unit "basalts–komatiites," it was recorded as such and indicated in the metadata for calculations that apply areal weighting.

2.2.4. Calculation of lithological averages and areal proportion

For each lithology/unit, the following were calculated: 1) the arithmetic mean and standard deviation for each oxide, and 2) the areal proportion by lithology in Gorgona when the unit had a known surface area in the geological maps. Considering that C_u is the mean value of unit u and $w_u$its corresponding area fraction (with $\Sigma_u w_u = 100\%$), the weighted mean composition of the island was obtained using eq. (5):

$$\underline{C}_{Gorgona\_pond} = \sum_u w_u C_u \quad (5)$$

This arithmetic and weighted mean values were explicitly stored, as they are used in the comparison strategy based on FOMc. It is worth noting, weighted mean values approach for estimating the composition of an area with multiple units and assessing petrological analogs, was also used in past studies (e.g. Nakhla - (old) Theo's Flow; Lentz et al., 1999).

2.3. Preparation of data subsets for specific metrics

From the main dataset, data subsets were generated consistent with each family of analyses in the comparative meta-analysis: 1) for FOMc, only compositions containing the complete common vector from main oxides were used; and 2) for geochemical ratios (e.g., Al_2O_3/TiO_2), samples reporting the required components were selected, with no missing values included in the ratios.

2.4. Geochemical ratios and Compositional Figures of Merit (FOMc)

Geochemical analyses were carried out to discriminate between magmatic styles and differentiation conditions. In particular, the Al_2O_3/TiO_2 ratio was employed, given that both oxides exhibit relatively immobile behavior during metamorphic or hydrothermal processes, making them robust indicators of the original composition (Arndt et al., 1997; Pearce, 2008). This ratio has been widely used to differentiate tectonic settings and to characterize partial melting and fractional crystallization processes (Lunning et al., 2017; Verma et al., 2017; Mendes et al., 2025). Although the purpose of this study is not to determine the genesis of the mafic rocks of Gorgona Island, understanding these relationships is relevant for the discussion. Additionally, an TAS and Jensen diagrams were plotted to establish whether the rocks are of tholeiitic or calc-alkaline affinity, with the aim of correlating them with their possible genesis, providing a general framework that facilitates the comparison of geochemical compositions of both materials. Additionally, both plots provide critical information regarding geochemical similarities between materials from Syrtis Major and Gorgona Island.

The calculation of FOMc was adopted in accordance with ISO 10788:2014 (Reference for quantitative measures for lunar simulants; ISO, 2014), which defines it as the degree to which a sample matches a reference value through the comparison of normalized compositional vectors. This metric ranges from 0 (total incompatibility) to 1 (complete match), allowing for the evaluation of similarity with the reference material (Sibille et al., 2006; Rickman et al., 2007, 2009).

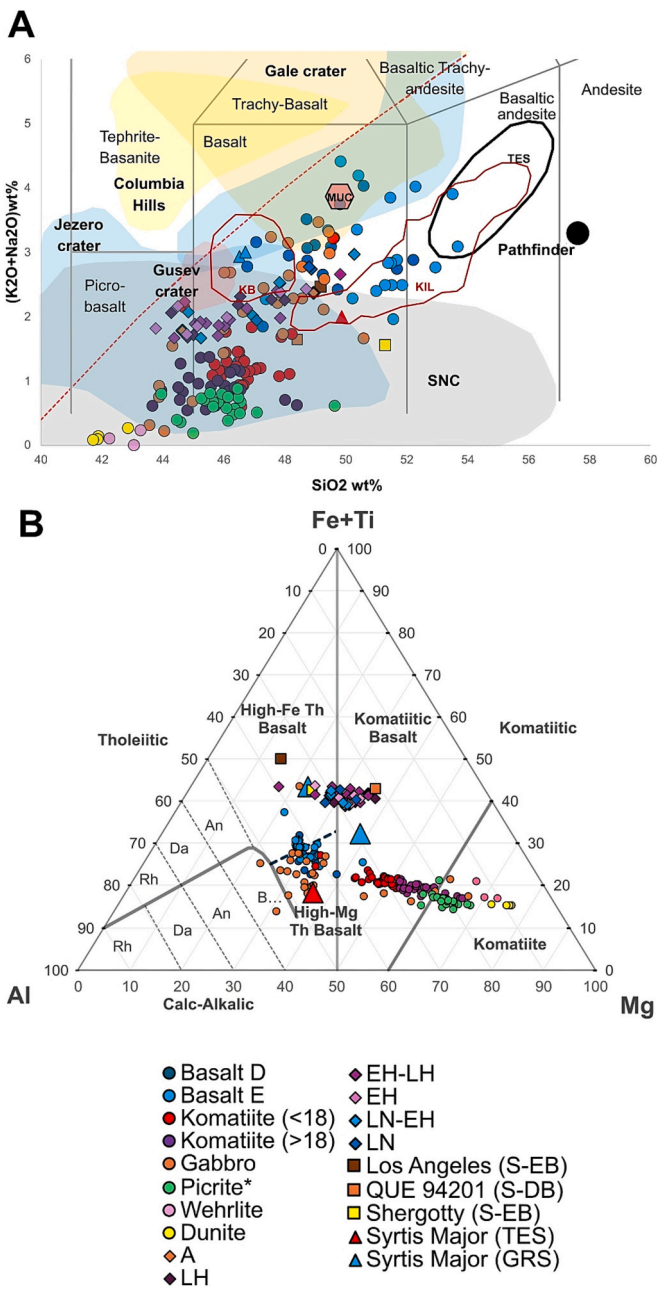

Fig. 6. TAS classification (Le Maitre et al., 2005) and Jensen Cation Ternary diagrams (Fe + Ti–MgO–Al_2O_3) (Jensen and Pyke, 1982) comparing compositions from Gorgona Island and Syrtis Major remote sensing metadata and meteorites data. [SINGLE COLUMN IMAGE].

In this study, geochemical composition was used for the FOMc analysis between the rocks of Gorgona and Syrtis Major, and the main major oxides (SiO_2, TiO_2, Al_2O_3, FeO_t, MgO, CaO, Na_2O, K_2O, P_2O_5, and MnO) were employed as comparison vectors. The FOMc between the compositions of the two sites (Gorgona and Mars) x and y was calculated using the following equation:

$$FoM_{xy} = 1 - \frac{\Sigma_i |X_{i,x} - X_{i,y}|}{\Sigma_i (X_{i,x} + X_{i,y})} \quad (6)$$

where $X_{i,x}$ and $X_{i,y}$, corresponds to the wt% fractions of oxide i in compositions x and y respectively. The value obtained in eq. (6) ranges between 0 and 1.

The FOMc analysis procedure was carried out in two ways: 1) comparisons of individual samples (Syrtis or SNC–Gorgona), followed by lithological averages; and 2) an island-scale integration weighted by the relative surface area of each geological unit as a means to assess analog terrain geochemical similarity as a whole, in which the average of the data by lithology in Gorgona was compared with the average of the data by geological period on Mars or the SNC.

In the case of individual sample comparisons, across the total set of similarity measures, the bootstrap resampling method was applied to estimate the mean and a 95% coverage interval from the distribution generated using 2000 samples in each case of interest, by the use of the R software (R Core Team, 2024). This was done considering that an initially non-normal distribution was observed. This method is characterized as a non-parametric technique that approximates the distribution of an estimator through resampling with replacement from the original data. This procedure allows for the estimation of confidence intervals and standard errors without assuming parametric distributions, making it essential in contexts with unknown or complex assumptions.

For the second type of FOMc analysis, average values and comparability percentages were calculated for each Gorgona Island's lithology (LC_u) or for each geological period unit (Mars) or SNC, as well as an integrated value for the island obtained through weighting by the surface area of each geological unit, based on the data of Serrano (2011) and Révillon (2000). This is a similar approach used by Lentz et al. (1999) for assessing Theo's Flow, an archean lava flow within Abitibi greenstone belt in Ontario, Canada, as an analog terrain for Martian lava flows or sills of Nakhlite meteorite composition (Friedman et al., 1995) and magmatic crystallization processes (Lentz et al., 2011). Lentz et al. (1991) not only assessed the geochemical similarities between Nakhlite meteorite and multiple individual lithologies (peridotite, pyroxenite and gabbro), but also the lithological layering of the 120 m thick flow by weighing each lithological composition according to its stratigraphic thickness, which was subsequently compared to Martian compositions (Table 3 and Fig. 9). This approach takes into consideration the diversity and relative abundance of geochemically similar (and dissimilar) lithological compositions of the study area and helps to constrain the extent and comparability of a given analog terrain.

To this end, our FOM criteria to determine the comparability of individual samples and potential analog terrains is based on the FOM values of established analogue terrains. For which we conducted a FOM analysis of Lentz et al. (1999) data and use the resulting FOM values as a benchmark for determining the degree of similarity between Gorgona island and Syrtis Major compositions (Supplementary Material 1). This value obtained from the comparison between the weighted composition of Theo's Flow and Nakhla meteorite corresponds to 0.88, which was used as lower limit to determine Gorgona Island's viability as a geochemical analog terrain. This value is consistent with the lower end compositional comparability of established Martian simulants, namely, Basic Martian simulant MMS-1 (Beegle et al., 2007; Peters et al., 2008) compared to average Gusev crater rock compositions (Scott et al., 2017) (FOM: 0.87; S3 Supplementary data from San Martin et al., 2025). It should be noted that simulant materials are more specialized in replicating compositional and physical properties of global, regional or local geologic extraterrestrial materials, which are made to represent said materials for engineering and astrobiological applications. These properties (e.g. geochemistry) are generally replicated with a higher degree of fidelity in comparison to terrestrial analogue materials (Ramkissoon et al., 2019), which are mostly based on relative mineralogical or petrological similarities (Dypvik et al., 2021).

3. Results

The compositional datasets analyzed in this study include orbital spectroscopic data from OMEGA, supplemented by previously published geochemical interpretations of Syrtis Major, as well as whole-rock geochemical data from Gorgona Island ultramafic and mafic units. All

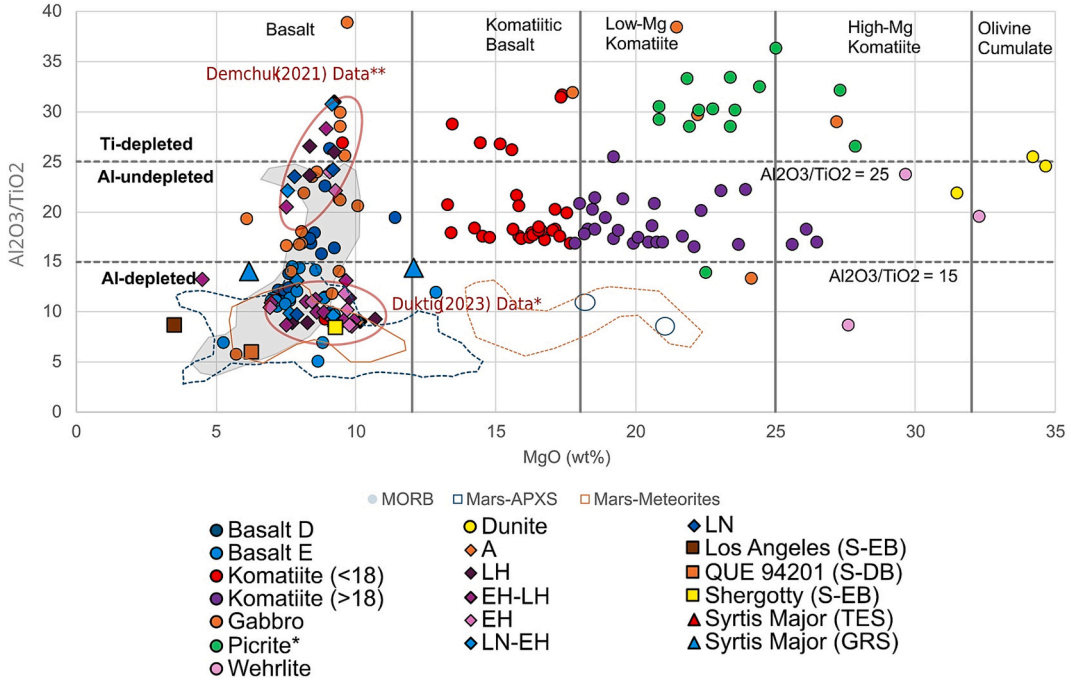

Fig. 7. (Al_2O_3/TiO_2) vs MgO plot showing the distribution of Gorgona Island's lithologies in comparison with Martian units (Late Noachian (LN), Early and Late Hesperian (EH, LH), Amazonian (A), and total average of Syrtis Major) and SNC meteorites. [DOUBLE COLUMN IMAGE].

datasets were standardized and expressed in terms of major oxide abundances to ensure comparability.

Following the methodology described in Section 3, compositional vectors were constructed using normalized oxide fractions. This normalization allows each sample to be represented within a multidimensional compositional space, enabling direct quantitative comparison between Martian surface materials and Gorgona Island lithology.

3.1. Geochemical analysis

The geochemical analysis integrates orbital datasets (TES, GRS, and OMEGA-derived interpretations), Martian meteorite compositions (SNC group), and data from Gorgona Island. All compositions were standardized using major oxide abundances and subsequently evaluated through normalized compositional vectors, enabling direct comparison across datasets.

The results indicate that Syrtis Major exhibits a predominantly mafic to ultramafic geochemical signature. In the MgO versus Al_2O_3/TiO_2 diagram (Fig. 7), the Martian datasets cluster within fields corresponding to basaltic and komatiitic compositions, with MgO values typically ranging between ~6 and 12 wt%, and Al_2O_3/TiO_2 ratios spanning both Al-depleted and transitional domains. These distributions overlap significantly with komatiitic basalts and low-Mg komatiites from Gorgona, suggesting comparable mantle-derived magmatic processes.

The ternary Fe–Ti–Mg diagram (Fig. 6B) further supports this interpretation, as Syrtis Major samples plot within the tholeiitic to komatiitic basalt fields, showing a clear affinity toward Mg-enriched compositions. Similarly, the SiO_2 versus total alkali diagram (Fig. 6A) indicates that most samples fall within basaltic and trachy-basaltic domains, with limited evidence of evolved compositions, reinforcing the interpretation of relatively primitive magmas.

The metadata compositions of Syrtis Major plotted in the TAS diagram shows adjusted, Fawdon (2015, 2016), Duktig (2023) and Demchuck (2021) datasets fall within the Jezero crater composition fields. The data also follows the field's trend with increasing SiO_2 and Alkali but is distinct due to lower alkali content (low K_2O GRS values). Gorgona Island mafic compositions (enriched and depleted basalts, and gabbros) follow Jezero crater trend and also fall within the compositional fields of two distinct terrestrial analog terrains (Kīlauea Volcano, Hawaii; King's Bowl & Wapi flows; Eastern Snake River Plain, Idaho, USA). Ultramafics are also included within the fields of SNC meteorites and Jezero crater compositions (Fig. 6A). Furthermore, Syrtis Major, ultra-mafic and mafic Gorgona compositions plotted in the Jensen cation ternary diagram shows a tholeiitic affinity for both compositions. Additionally, Martian compositions cluster in-between High-FeO basaltic and Komatiitic basalt compositions reflecting typical iron enrichment of Martian rocks in comparison with terrestrial samples (Fig. 6B). In contrast, the lithologies of Gorgona Island display a broader dispersion, ranging from komatiites to high-Mg Basalts (following primarily a trend from proportionally high MgO to High Al_2O_3 content) (Fig. 7).

The Al_2O_3 vs. TiO_2 bivariate diagram shows that the rocks of Gorgona Island span a wide range of values, mostly between 7.5 and 20 wt% Al_2O_3 and 0.2–1.5 wt% TiO_2 (Fig. 7). Basalts and komatiites display the greatest dispersion, whereas gabbros, picrites, dunites, and wehrlites tend to cluster within narrower intervals. The Martian values (Syrtis Major and SNC meteorites) partially overlap with those of Gorgona, with the strongest matches corresponding mainly to high–MgO komatiites and, to a lesser extent, to low–MgO komatiites. The compositions from different Martian epochs in the Syrtis Major region (Late Noachian to Amazonian) group within intermediate Al_2O_3 ranges (8.5–13 wt%). However, there is a clear difference between Demchuk (2021) and Duktig (2023) datasets, which reflect the original TiO_2 concentration (Lower TiO_2) from Remote sensing analysis and TiO_2 concentrations derived from Meteorite data (Higher TiO_2), respectively. This difference shows Ti-enriched Al-depleted and Al-enriched trends with the latter coinciding with Gorgona komatiite (>18% MgO) and Picrite lithologies. Additionally, a positive slope is observed for both Gorgona Island and Martian data, consistent with differentiation processes in rocks that concentrate TiO_2 while retaining Al_2O_3.

When analyzing these relations with MgO content, both datasets fall within the basalt field and coincide with MORB compositions. However, in this case only Duktig's (2023) Al-depleted Ti-enriched compositions fall within general Mars in-situ and meteorite compositions and coincide with most Gorgona Island's depleted basalts. High-MgO Martian

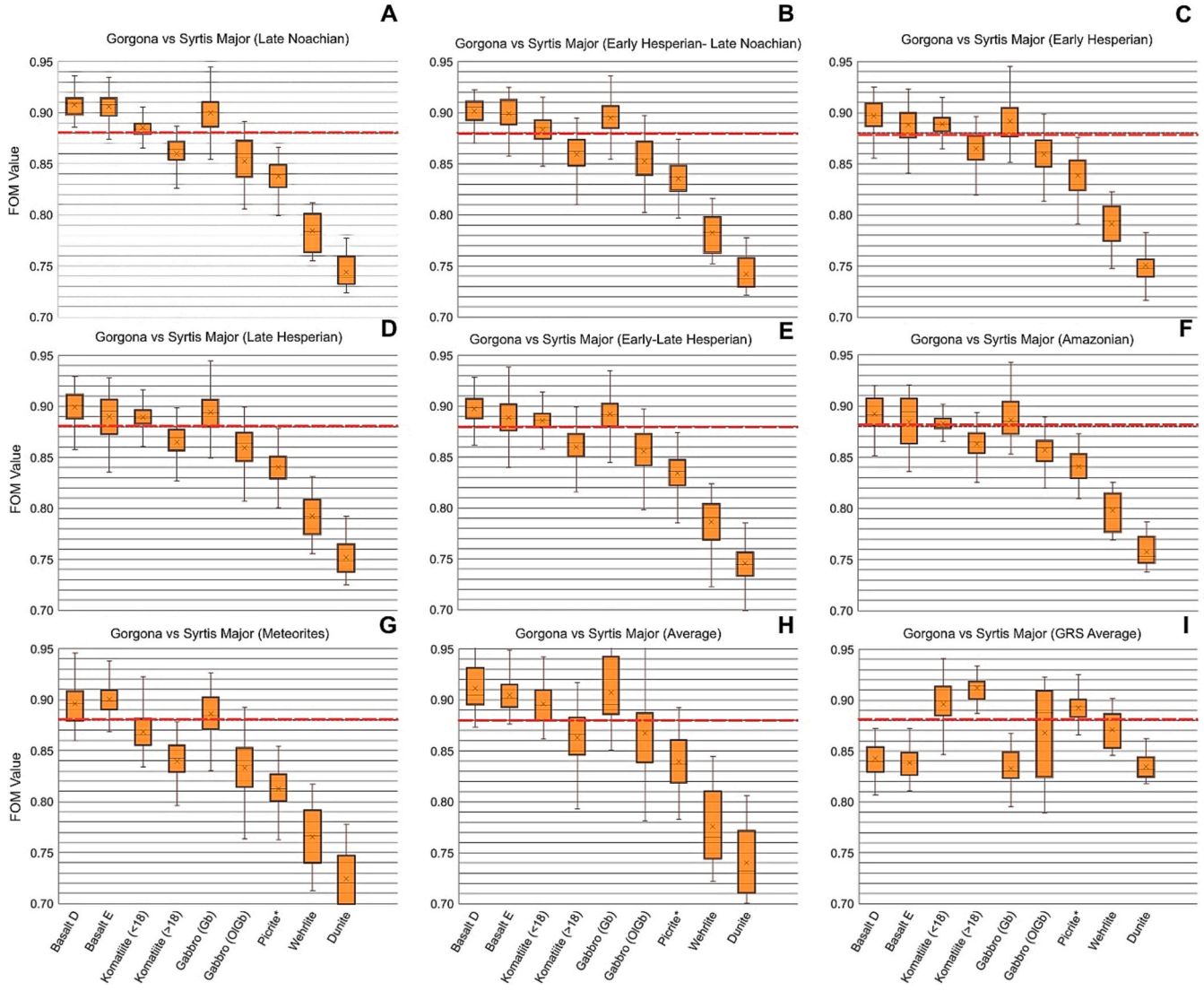

Fig. 8. Individual Compositional Figures of Merit (FOMc) for the lithologies of Gorgona compared with: A) Late Noachian, B) Early Hesperian-Late Noachian, C) Early Hesperian, D) Late Hesperian, E) Early Hesperian-Late Hesperian, F) Amazonian, G) Meteorites, H) Syrtis Major TES, I) Syrtis Major GRS. Data from Fawdon (2016), Demchuck (2021), and Duktig (2023). The red line indicates the similarity threshold. [DOUBLE COLUMN IMAGE]. (For interpretation of the references to colour in this figure legend, the reader is referred to the web version of this article.)

compositions also show Al-depletion in contrast to Gorgona Al-undepleted komatiites.

3.2. *Compositional figures of merit (FOMc): Individual analyses*

.The compositional similarity between Syrtis Major and Gorgona Island lithologies was quantitatively evaluated using the Compositional Figures of Merit (FOMc), calculated from normalized compositional vectors as described in Section 3. This approach enables a direct assessment of geochemical affinity by measuring the normalized distance between samples in multidimensional oxide space, where lower distances (and thus higher FOMc values) indicate stronger compositional similarity.

Quantitative comparison using Figures of Merit (Fig. 8) reveals consistently high similarity values between Syrtis Major and mafic to ultramafic lithologies, particularly basalts, komatiitic basalts, and gabbroic compositions, which typically exhibit FOM values above ~0.88 across multiple geological periods. In contrast, more evolved or highly differentiated lithologies, such as wehrlites and dunites, display lower similarity values (generally <0.80), indicating reduced compositional agreement.

Across all temporal subsets of Syrtis Major (Late Noachian to Amazonian; Fig. 8A–F), mafic lithologies, particularly basaltic and komatiitic compositions, consistently yield the highest FOMc values, generally exceeding ~0.88. Basalt D and Basalt E, as well as komatiites (<18 wt% MgO), display median FOMc values commonly ranging between ~0.89 and 0.92, with relatively low dispersion, indicating a stable and robust compositional match. Gabbroic compositions (Gb and OlGb) also exhibit comparably high FOMc values, typically between ~0.87 and 0.91, further supporting a coherent mafic affinity.

In contrast, ultramafic end-members such as wehrlites and dunites systematically show lower FOMc values, generally below ~0.80, with medians often between ~0.73 and 0.79. This indicates a reduced compositional agreement with Syrtis Major, suggesting that although ultramafic components may be present, they do not dominate the bulk geochemical signature. Picritic compositions occupy an intermediate position, with FOMc values typically between ~0.82 and 0.86, reflecting partial but not optimal correspondence.

The consistency of these patterns is preserved across independent datasets, including Martian meteorites (Fig. 8G), averaged compositions

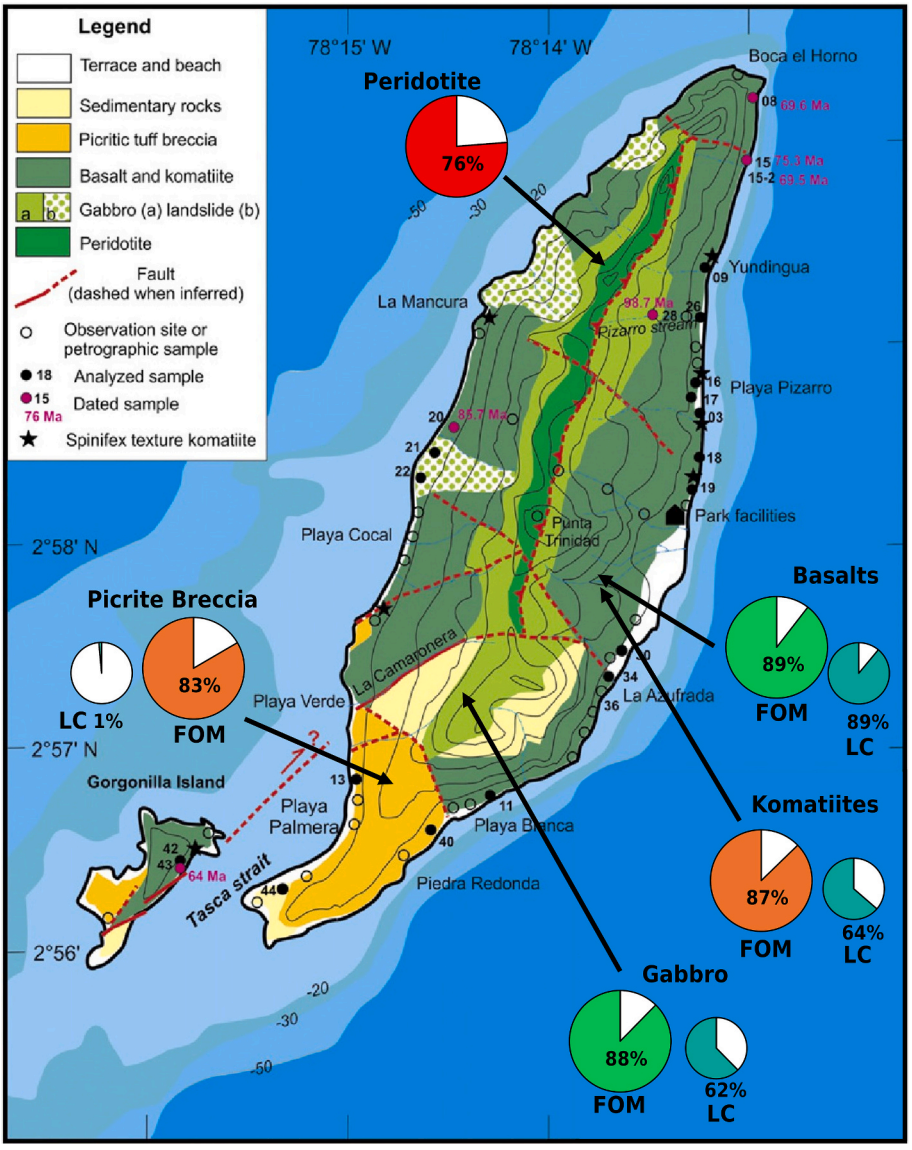

Fig. 9. Geological map of Gorgona Island modified from Serrano et al. (2011), showing the spatial distribution of the main lithological units, including peridotites, basalts and komatiites, gabbroic bodies, and picritic breccias. The map also indicates structural features such as faults, sampling locations, and dated sites. Superimposed pie charts represent the Compositional Figures of Merit (FOM) and lithological coverage (LC) for each unit: basalts (FOM ~89%, LC ~89%), komatiites (FOM ~87%, LC ~64%), gabbros (FOM ~88%, LC ~62%), picritic breccias (FOM ~83%, LC ~1%), and peridotites (FOM ~76%). [SINGLE COLUMN IMAGE].

Table 3
Areal distribution of the main lithologies of Gorgona Island according to Serrano et al. (2011) and Révillon et al. (2000).

Geological units	Serrano et al. (2011)		Révillon et al. (2000)	
	Surface area (km^2)	Percentage (%)	Surface area (km^2)	Percentage (%)
Basalts & Komatiites	4168	42,3%	6197	54,80%
Gabbros	3.502*	35,6%	3,16	27,90%
Picrites	1.275	13,0%	1.17	10,30%
Dunites & Wherlites	8.957	9,1%	7.85	7,00%
Total	9.832	100%	11.311	100,00%

(Fig. 8H), and GRS-derived data (Fig. 8I). Notably, komatiitic and basaltic compositions maintain high FOMc values across all datasets, reinforcing the reproducibility of the results. While slight variations in dispersion are observed, particularly in averaged datasets, these do not significantly alter the overall ranking of lithological affinity.

Importantly, the observed FOMc distributions remain stable through geological time. From the Late Noachian to the Amazonian, basaltic and komatiitic compositions consistently exhibit the highest similarity values, indicating that the dominant geochemical signature of Syrtis Major has remained largely unchanged. This temporal persistence suggests long-lived magmatic processes characterized by mafic to moderately ultramafic compositions.

Overall, the FOMc analysis demonstrates that Syrtis Major is best represented by basaltic to komatiitic compositions, with strong and reproducible affinity across multiple datasets and geological periods. The comparability of high FOMc values for these lithologies, combined with their low dispersion, supports a robust interpretation of Syrtis Major as a mafic-dominated volcanic province with contributions from primitive mantle-derived magmas.

3.3. Compositional figures of merit (FOMc): Analyses with mean values and areal proportion

To further constrain the compositional affinity between Syrtis Major and Gorgona Island materials, the FOMc analysis was extended using mean compositions weighted by areal proportions of lithological units. This approach provides a more representative assessment of bulk crustal composition by integrating both geochemical similarity and spatial dominance, as described in previous subsections.

The results reveal a clear shift in interpretation compared to individual analyses. While ultramafic lithologies such as komatiites and picritic units exhibit relatively high FOMc values when considered independently (typically ~0.83–0.88). In contrast, basaltic units, characterized by both high FOMc values (~0.88–0.90) and dominant spatial distribution. Gabbroic lithologies also show consistently high FOMc values (~0.87–0.89) and moderate areal representation, reinforcing their relevance as part of the dominant mafic framework. Conversely, peridotitic units, despite representing a substantial local proportion (up to ~76% in specific sectors), display comparatively lower FOMc values (Fig. 9).

Overall, the combined FOMc and areal proportion analysis indicates that Syrtis Major is best represented by a basalt-dominated compositional framework, with contributions from komatiitic and gabbroic units. This result provides a more realistic approximation of crustal composition and strengthens the interpretation of Syrtis Major as a mafic volcanic province with localized ultramafic signatures rather than a dominantly ultramafic system.

The mean values of major oxides calculated for different geological period units of Mars in the Syrtis Major region, the Syrtis Major average, and SNC meteorites yielded consistently high FOMc values (Fig. 8). The highest values correspond to the Late Hesperian (0.900–0.898), followed by the Early Hesperian (0.899–0.896) and the Late Noachian (0.899–0.889). Syrtis Major shows a mean value of 0.891, whereas the SNC meteorites range between 0.895 (QUE 94201) and 0.861 (Los Angeles).

The weighting of Gorgona Island's lithologies by areal proportion (Table 3) shows that basalts and komatiites account for between 42.3% (Serrano et al., 2011) and 54.8% (Révillon et al., 2000) of the island's surface, followed by gabbros (27.9–35.6%), picrites (10.3–13.0%), and dunites–wehrlites (7.0–9.1%), respectivley. Considering these percentages, mafic rocks (basalts and gabbros), together with komatiites, have the greatest weight in compositional similarity with Mars, whereas picrites, dunites, and wehrlites contribute to a lesser extent.

4. Discussion

4.1. Mafic to ultramafic affinity of Syrtis Major

The integrated geochemical datasets indicate that Syrtis Major is predominantly characterized by mafic compositions with subordinate ultramafic contributions. Major element systematics (Fig. 6A) show that most samples cluster within basaltic and trachy-basaltic fields, with limited evidence for evolved compositions. Similarly, the Fe–Ti–Mg ternary diagram (Fig. 6B) places the data within tholeiitic to komatiitic basalt domains, suggesting relatively primitive mantle-derived magmas.

The Al_2O_3/TiO_2 versus MgO relationships (Fig. 7) further constrain these compositions, spanning basaltic, komatiitic basalt, and low-Mg komatiite fields. The presence of Al-depleted to transitional signatures indicates variable degrees of partial melting and source heterogeneity. The Al_2O_3/TiO_2 vs. MgO relationships show that Martian compositions fall largely within the Al-depleted to moderately Al-undepleted fields, mirroring the trends observed in Gorgona Island's komatiites (>18 wt% MgO) and depleted basalts. This is also consistent with fractionation dominated by pyroxene ± olivine and is comparable to MORB-like differentiation pathways.

Syrtis Major geochemical signatures also reinforce the genetic similarities in the planetary formation of Martian (e.g. Tharsis & Elysium Volcanic provinces) and terrestrial (e.g. Oceanic Crust & Hot spot volcanism) secondary crusts (Taylor, 2009), and the link between terrestrial oceanic crust MORB/OIB and Martian Meteorites (Greenough and Ya'acoby, 2013; Gross et al., 2013;Putirka, 2016; Filiberto, 2017, 2019; Day et al., 2018) and Martian (In-Situ) compositions (Ray and Misra, 2015).

Collectively, these observations support a compositional continuum dominated by mafic magmas with contributions from more primitive melts, rather than discrete lithological end-members.

The TAS diagram reinforces this affinity, with Syrtis Major plotting near Jezero crater data and near areas (Brown et al., 2020; Fawdon et al., 2015; Liu et al., 2022; Tosca et al., 2025) and within terrestrial analog fields that Gorgona Island also occupies, particularly along the low-alkali basaltic trend. This reflects a shared geochemical architecture dominated by low-alkali, Fe-rich magmas.

Moreover, the Al_2O_3/TiO_2 ratio (Fig. 7) shows compositional matches between both regions. Syrtis Major, together with SNC meteorites, plots within a range of 8–15 wt% Al_2O_3 and 0.3–1.0 wt% TiO_2, an interval that coincides with the basalts and komatiites of Gorgona Island.

Collectively, these observations support a compositional continuum dominated by mafic magmas with contributions from more primitive melts, rather than discrete lithological end-members.

4.2. Consistency across independent datasets

A key outcome of this study is the strong agreement among independent datasets, including orbital observations (TES, GRS, OMEGA-derived interpretations), Martian meteorites, and terrestrial analog compositions. This comparability is evident across geochemical diagrams and is quantitatively supported by the FOMc analysis (Fig. 8A-8F): Basaltic, gabbroic, and komatiitic (particularly <18 wt% MgO) lithologies consistently yield high FOMc values (≥0.88) across all geological periods, while also exceed similarity thresholds. Importantly, these patterns persist from the Late Noachian through the Amazonian, indicating that the compositional signal is robust and not dependent on a specific dataset or analytical approach.The agreement between orbital and meteoritic data further suggests that these signatures reflect primary crustal compositions rather than localized alteration or surface processes.

4.3. From compositional similarity to bulk crustal representation

The integration of FOMc analyses based on individual samples and areal-weighted compositions provides critical insight into the representativeness of different lithologies. While individual analyses (Fig. 8A–8F) indicate high compositional similarity between Syrtis Major and both mafic and ultramafic lithologies, the incorporation of areal proportions significantly refines this interpretation.

In all cases, enriched and depleted basalts and gabbros yield FOMc values >0.88. Moreover, for the Syrtis Major regions corresponding to the Early Hesperian, Late Hesperian, and the overall Syrtis Major average, komatiites with <18% MgO also exceed the defined threshold for compositional analogy. By contrast, dunites and wehrlites display the lowest values, consistent with the absence of equivalent lithologies in Martian datasets for this region. In relation with SNC meteorites, Los Angeles and Shergotty enriched basalts scored below the FOM limit (FOMc ≈ 0.84–0.85). on the other hand, QUE 94201 depleted basalt showed more overall compatibility with Gorgona Terrain (FOMc ≈ 0.87), with a Gorgona Island's depleted basalts reaching an average FOMc value of 0.90. It is worth noting that both Poulet et al. (2009), Los Angeles and Shergotty SiO_2 values are outside the compositional range provided by GRS data. Although the lithologies associated with Gorgona's mafic and ultramafic rocks show the greatest similarity not only in composition but also in genetic affinity with the materials detected in

Syrtis Major, the possible presence of gabbros on Mars is not unexpected according to Cousin et al. (2017), Fawdon et al. (2015), and Filiberto et al. (2014).

The FOMc analysis based on mean values and areal proportion (Fig. 8, Fig. 9, and Table 3) complements this interpretation.

The geological map of Gorgona highlights the analogies of the combined evaluation of compositional similarity (FOM) and spatial representativeness. Here, LC (Lithological Coverage) refers to the proportion of the mapped area occupied by each lithological unit, providing a measure of its spatial significance within the system. Basalts emerge as the most robust unit, with both high compositional agreement (FOM ~89%) and dominant areal coverage (LC ~89%), indicating that the best compositional match is also the most representative lithology. Komatiites (FOM ~88%, LC ~64%) and gabbros (FOM ~88%, LC ~62%) also show strong compositional affinity but with more restricted distribution, suggesting an important yet secondary contribution to the overall analogue. In contrast, picritic breccias (FOM ~83%, LC ~1%) are spatially negligible despite good compositional agreement, while peridotites (FOM ~76%) display lower compositional affinity overall. These relationships demonstrate that the analogue is best understood as an integrated basalt–komatiite–gabbro system, where both compositional fidelity and spatial dominance must be considered.

4.4. Implications for magmatic processes in Syrtis Major

The geochemical characteristics identified here are consistent with high-temperature magmatic processes involving substantial degrees of mantle partial melting (Arndt et al., 1997; Filiberto, 2014). The presence of Mg-rich compositions and komatiitic affinities suggests that Syrtis Major magmas were derived from relatively hot mantle sources, particularly during earlier stages of crustal formation (Baratoux et al., 2014; Mustard et al., 2005). The association between Mg-rich compositions and elevated mantle temperatures is well supported. High Mg values, abundant olivine, and primitive basaltic compositions identified in Syrtis Major are widely interpreted as evidence for high degrees of partial melting, which in turn imply relatively Thermal evolution models of Mars further support the idea that mantle potential temperatures were higher in the early planet, enabling the generation of primitive, Mg-rich melts (Filiberto 2014). In this sense, the inference of relatively hot mantle sources is robust.hot mantle conditions, particularly during the Noachian–Hesperian transition.

The coexistence of basaltic and more primitive compositions likely reflects variations in melt extraction, fractional crystallization, and mantle source heterogeneity. Such variability is consistent with prolonged volcanic activity and may be compatible with plume-related magmatism, although additional geophysical constraints are required to evaluate this hypothesis (Arndt et al., 1997; Filiberto and Dasgupta, 2015).

The potential presence of komatiites on Mars is grounded in the planet's early thermal state and the geochemical characteristics of its most primitive magmas. Thermal evolution models indicate that early Mars likely had higher mantle potential temperatures than present-day Earth, particularly during the Noachian and early Hesperian, due to rapid accretion, radiogenic heating, and inefficient heat loss (Filiberto and Dasgupta, 2015). Under such conditions, high degrees of partial melting (>30–40%) could have been achieved, which are comparable to those required for komatiite generation on Archean Earth (Arndt et al., 1997).

his thermal framework is supported by observations of Mg-rich, olivine-dominated lithologies in regions such as Syrtis Major, where spectral data reveal compositions consistent with primitive, high-temperature melts (Mustard et al., 2005). The presence of extensive, low-viscosity lava flows and fissure-fed plains volcanism further aligns with emplacement styles expected for ultramafic magmas. Additionally, Martian meteorites (e.g., olivine-phyric shergottites) record high Mg# and evidence for relatively deep, hot mantle sources, reinforcing the plausibility of generating komatiite-like melts (Treiman, 2003).

Importantly, Mars' lower gravity and lack of plate tectonics may have facilitated the ascent and preservation of such primitive melts without extensive crustal reprocessing, increasing the likelihood that komatiitic compositions could reach and be preserved at the surface. Therefore, while direct identification remains challenging, converging lines of thermal, geochemical, and volcanic evidence support the feasibility of komatiite formation on early Mars, particularly in Syrtis Major.

4.5. Implications for Martian crustal evolution

These results support a model in which the Martian crust, at least in regions such as Syrtis Major, is dominated by mafic compositions with localized contributions from more primitive magmas. The presence of komatiitic affinities suggests that early Martian mantle conditions were sufficiently hot to generate high-Mg melts, analogous to those observed in early terrestrial environments.

The consistency of these signatures from the Noachian to the Amazonian indicates that Syrtis Major preserves key characteristics of early mantle-derived magmatism. This implies that crustal formation on Mars was largely controlled by sustained basaltic volcanism, with intermittent contributions from higher-degree partial melts.

At a broader scale, these findings are consistent with models linking Martian crustal compositions to MORB- and OIB-like processes, suggesting fundamental similarities in mantle melting dynamics between Earth and Mars despite differing tectonic regimes.

These coincidences and contrasts have implications in three key aspects:

1. Geochemically speaking, the data suggests that Syrtis Major preserves poorly differentiated magmas, generated at high temperatures and with low viscosity, comparable to those of Gorgona Island and similar lithologies (e.g. Barberton, Pilbara) (Arndt et al., 1997; Filiberto, 2014). The emplacement of high-temperature, mafic and ultramafic lavas on Earth, is a manifestation of mantle dynamics, reflecting high degrees of partial melting (>15%) and the activity of deep thermal anomalies such as mantle plumes or superplumes (Campbell and Griffiths, 1990; Herzberg et al., 2010; Putrika, 2016). These magmatic events, often linked to rifting and large igneous provinces, mark episodes of elevated heat flux and vigorous mantle convection along with low-viscosity magmas that facilitates rapid ascent and extensive effusion, influencing crustal stability and differentiation (Campbell and Griffiths, 1990; Koppers et al., 2021; Richards et al., 1989). Consequently, such eruptions provide critical insights into the planet's early thermal state, the evolution of mantle composition, and the tectonomagmatic mechanisms governing lithospheric development.
2. In terms of planetary processes, they reinforce the hypothesis that Syrtis Major volcanism corresponds to Martian secondary crust magmatism and possesses magmatic processes similar to terrestrial Oceanic crust MORB/OIB magmatism (terrestrial genetic tectonic processes are not implied). The product of a heterogeneous mantle capable of generating both enriched and depleted magmas over time, includes high-temperature magmas such those implied in basalts and komatiites formation (Hiesinger & Head, 2004; Lillis et al., 2015; Black et al., 2016).
3. Finally, astrobiological implications related to the presence of ultramafic rocks on Mars implies the potential for underground serpentinization processes capable of producing H_2 and CH_4, reducing gases with the capacity to sustain primitive microbial communities (McCollom and Seewald, 2013; Shimizu et al., 2009). Remarkably, evidence of serpentinization was confirmed by in-situ detection in the NE region of Syrtis Major/SE of Nili Fossae in Jezero crater (Tosca et al., 2025), and Serpentine mineral signatures were detected NW, SW and the southern edge of Syrtis Major (and other Noachian and Hesperian terrains) by orbital CRISM with high confidence

(Emran et al., 2025). Along with Jezero crater, this makes the Syrtis Major region an important target for astrobiological research.

4.6. Relevance of Gorgona Island as a terrestrial analog

The comparison with Gorgona Island provides a robust framework for interpreting the compositional and petrogenetic characteristics of Syrtis Major. Geochemical diagrams (TAS, Jensen, Al_2O_3/TiO_2 vs MgO) show substantial overlap between Syrtis Major data and Gorgona lithologies, particularly basalts, komatiitic basalts, and gabbros (Fig. 6 and Fig. 7).

FOMc analyses reinforce this similarity, with the highest values consistently associated with these lithologies (Fig. 8). However, areal-weighted results (Fig. 9 and Table 3) indicate that, as in Syrtis Major, the bulk compositional signal in Gorgona is dominated by mafic rocks despite the presence of ultramafic units.

This combined compositional and spatial agreement supports the use of Gorgona as a terrestrial analog, capturing the coexistence of primitive and evolved mafic systems within a single volcanic province. As such, it provides a useful reference framework for interpreting mantle-derived magmatism and crustal development on Mars.

Beyond affinities, the differences are equally instructive. The extreme ultramafic lithologies of Gorgona Island show no clear correlation with the available Martian data, suggesting that Mars may not have generated MgO-rich magmas such as those preserved on the island. Nevertheless, this lithological diversity makes Gorgona Island a natural catalog encompassing a wide spectrum of magmatic scenarios, thereby providing a broader comparative framework than other terrestrial igneous provinces (Kerr, 2005). Such similarities and discrepancies are inherent to the nature of analogs, since no location on Earth perfectly replicates the characteristics reported on Mars.

The compositional comparability between Gorgona Island and Syrtis Major, from a geological standpoint, provides a natural laboratory for investigating plume-related magmatism, high-temperature mantle melting, and crustal differentiation under oxidizing conditions analogous to those inferred for Syrtis Major. Detailed mineralogical, isotopic, and textural studies could refine our understanding of the thermodynamic parameters that governed magma evolution on both planets. Integrating high-resolution techniques will allow quantifying subtle variations in Fe—Mg exchange and volatile contents relevant to Martian processes. In parallel, hydrothermal alteration experiments on Gorgona Island's ultramafic and mafic rocks could simulate serpentinization pathways capable of producing H_2 and CH_4, gases with direct astrobiological significance. Such studies would clarify the role of water–rock interactions in generating redox gradients that could sustain chemosynthetic life. Ultimately, combining petrological, geochemical, and mineralogical analyses from terrestrial analogs like Gorgona Island with current and future datasets from CRISM, PIXL, and SHERLOC will enable a more integrated perspective on Mars' magmatic evolution, crustal dynamics, and potential habitability across geological time.

Looking ahead, it will be necessary to expand the geochemical database of Gorgona Island using high-resolution techniques (e.g. Raman spectroscopy), as well as to take advantage of the most recent Martian datasets acquired by instruments such as CRISM, PIXL, and SHERLOC. Likewise, investigating hydrothermal alteration processes in Gorgona Island ultramafic rocks may provide key insights into the habitability of analogous environments on Mars, offering a valuable framework for future studies in astrobiology (e.g. past Martian habitability, as water–rock interactions that may have generated redox gradients and energy sources capable of sustaining potential microbial life).

5. Conclusions

- This study integrates orbital geochemical data, Martian meteorites, and terrestrial analogs to quantitatively assess the compositional nature of Syrtis Major and its relationship to mafic and ultramafic lithologies.
- The results demonstrate that Syrtis Major is predominantly characterized by mafic compositions, with consistent contributions from moderately primitive, Mg-rich magmas. Major element systematics and geochemical diagrams (TAS, Jensen, and Al_2O_3/TiO_2 vs MgO) indicate that these compositions define a continuum spanning basaltic to komatiitic basalt domains, rather than discrete lithological end-members.
- The FOMc analysis provides quantitative support for this interpretation, showing that basaltic and gabbroic lithologies systematically yield the highest similarity values across all geological periods. Komatiitic compositions also exhibit significant affinity, although their contribution is more limited when spatial representativeness is considered. Areal-weighted analyses further demonstrate that basaltic units dominate the bulk compositional signal, highlighting the importance of integrating spatial distribution with geochemical similarity.
- The strong agreement among independent datasets, including orbital observations, and meteorites, indicates that the observed compositional trends are robust and likely reflect primary crustal characteristics. These results support a model in which Syrtis Major formed through sustained mantle-derived magmatism, involving relatively high degrees of partial melting and limited evolution toward felsic compositions.
- The comparison with Gorgona Island reinforces this interpretation, as both regions exhibit overlapping compositional fields and similar distributions of mafic-dominated lithologies with subordinate ultramafic components. This supports the use of lithological units from Gorgona Island as a relevant terrestrial analog for interpreting Martian volcanic provinces, as well as useful location for investigations regarding to planetary geology and astrobiology.
- Overall, this study provides quantitative evidence that the crust of Syrtis Major is dominated by mafic compositions with localized ultramafic contributions, consistent with mantle-driven magmatism under relatively high thermal conditions. These findings contribute to a broader understanding of Martian crustal evolution and support the existence of compositional affinities between Martian volcanic provinces and terrestrial oceanic crust analogs, and astrobiological settings that might be explored by future planetary missions to Mars.

Availability of data and materials

All the data generated or analyzed during this study are included in this published article.

CRediT authorship contribution statement

D. Tovar: Writing – review & editing, Writing – original draft, Visualization, Investigation, Conceptualization. **M.A. Leal:** Writing – review & editing, Writing – original draft, Visualization, Investigation, Conceptualization. **M.A. de Pablo:** Writing – review & editing, Writing – original draft, Visualization, Investigation, Conceptualization. **J. San Martin-Lobos:** Writing – review & editing, Formal analysis, Data curation. **N. Tchegliakova:** Writing – review & editing. **F. Vélez:** Formal analysis, Data curation. **A. Molina:** Writing – review & editing. **G. Leone:** Writing – review & editing. **J. Sánchez:** Writing – review & editing. **A. Torres:** Writing – review & editing. **M.A. Bonilla:** Writing – review & editing. **R. Acevedo-Barrios:** Writing – review & editing. **G. Cancino-Escalante:** Writing – review & editing.

Statements and declarations

The authors declare that they have no known competing financial interests or personal relationships that could have appeared to influence the work reported in this paper.

Funding

The development of this project was made possible through funding obtained from Call 890–2020 of the Ministry of Science, Technology and Innovation of Colombia (MinCiencias), in support of the project "Assessment of the ecological, geological, geochemical, and climatological characteristics of Gorgona Island and the Nevado del Ruíz Volcano as terrestrial analogs of Mars and their potential for habitability and the development of analog missions." Jose San Martin is financed by the Europa¨ischen Sozialfonds (ESF) Plus in Sachsen, Germany under the project (SAB-Antragsnummer: 100670490) "Development of simulants for lunar regolith for research and development of in-situ resource utilization technology in Saxony". Additional resources and contributions were also provided by the institutions to which the authors are affiliated.

Declaration of competing interest

The authors declare that they have no conflicts of interest.

Acknowledgments

The authors would like to thank the institutions with which they work and collaborate (Corporación Científica LAGUNA, Grupo de Ciencias Planetarias y Astrobiología – GCPA, Universidad Nacional de Colombia, Universidad de Alcalá, Technische Universität Bergakademie Freiberg, Centro de Astrobiología - CAB, Universidad de Atacama, Instituto Tecnológico Metropolitano de Medellín, Universidad Tecnológica de Bolívar, Universidad de Pamplona), as their support has been essential for the development of this publication. The authors also express their gratitude to the Ministry of Science, Technology and Innovation of Colombia (MinCiencias) for supporting the project "*Assessment of the ecological, geological, geochemical, and climatological characteristics of Gorgona Island and the Nevado del Ruíz Volcano as terrestrial analogs of Mars and their potential for habitability and the development of analog missions*," funded under Call 890–2020. We are grateful to the anonymous reviewers whose perceptive comments guided us toward a stronger, clearer manuscript.

Appendix A. Supplementary data

Supplementary data to this article can be found online at https://doi.org/10.1016/j.icarus.2026.117133.

Data availability

The data used have been included as a supplementary file.

References

Aitken, B.G., Echeverría, L.M., 1984. Petrology and geochemistry of komatiites and tholeiites from Gorgona Island, Colombia. Contrib. Mineral. Petrol. 86 (1), 94–105. https://doi.org/10.1007/BF00373714.

Arndt, N.T., Naldrett, A.J., Pyke, D.R., 1977. Komatiitic and iron-rich tholeiitic lavas of Munro township, Northeast Ontario. J. Petrol. 18 (2), 319–369. https://doi.org/10.1093/petrology/18.2.319.

Arndt, N.T., Kerr, A.C., Tarney, J., 1997. Dynamic melting in plume heads: the formation of Gorgona komatiites and basalts. Earth Planet. Sci. Lett. 146 (1–2), 289–301. https://doi.org/10.1016/S0012-821X(96)00219-1.

Arndt, N., Lesher, M.C., Barnes, S.J., 2008. Komatiite. Cambridge University Press, p. 487.

Bandfield, J.L., 2002. Global mineral distributions on mars. J. Geophys. Res. Planets 107 (E6). https://doi.org/10.1029/2001JE001510, 9–1.

Baratoux, D., Toplis, M.J., Monnereau, M., Gasnault, O., 2011. Thermal history of mars inferred from orbital geochemistry of volcanic provinces. Nature 472, 338–341. https://doi.org/10.1038/nature09903.

Baratoux, D., Samuel, H., Michaut, C., Toplis, M.J., Monnereau, M., Wieczorek, M., Garcia, R., Kurita, K., 2014. Petrological constraints on the density of the Martian crust. J. Geophys. Res. Planets 119, 1707–1727. https://doi.org/10.1002/2014JE004642.

Beegle, L.W., Peters, G.H., Mungas, G.S., Bearman, G.H., Smith, J.A., Anderson, R.C., 2007. Mojave martian simulant: a new martian soil simulant. In: Lunar and Planetary Science Conference, p. 2005.

Bibring, J.-P., 2005. Mars surface diversity as revealed by the OMEGA/Mars express observations. Science 307 (5715), 1576–1581. https://doi.org/10.1126/science.1108806.

Black, B.A., Manga, M., 2016. The eruptibility of magmas at Tharsis and Syrtis Major on Mars. J. Geophys. Res. Planets 121 (6), 944–964. https://doi.org/10.1002/2016JE004998.

Brown, A.J., Viviano, C.E., Goudge, T.A., 2020. Olivine-carbonate mineralogy of the Jezero crater region. J. Geophys. Res. Planets 125 (3). https://doi.org/10.1029/2019JE006011 e2019JE006011.

Brügmann, G.E., Arndt, N.T., Hofmann, A.W., Tobschall, H.J., 1987. Noble metal abundances in komatiite suites from Alexo, Ontario and Gorgona Island, Colombia. Geochim. Cosmochim. Acta 51, 2159–2169. https://doi.org/10.1016/0016-7037(87)90265-1.

Campbell, I.H., Griffiths, R.W., 1990. Implications of mantle plume structure for the evolution of flood basalts. Earth Planet. Sci. Lett. 99 (1–2), 79–93. https://doi.org/10.1016/0012-821X(90)90072-6.

Chevrier, V., Mathé, P.E., 2007. Mineralogy and evolution of the surface of mars: a review. Planet. Space Sci. 55 (3), 289–314. https://doi.org/10.1016/j.pss.2006.05.039.

Christensen, P.R., Bandfield, J.L., Clark, R.N., Edgett, K.S., Hamilton, V.E., Hoefen, T., Smith, M.D., 2000. Detection of crystalline hematite mineralization on Mars by the Thermal Emission Spectrometer: evidence for near-surface water. J. Geophys. Res. Planets 105 (E4), 9623–9642. https://doi.org/10.1029/1999JE001093.

Christensen, P.R., Bandfield, J.L., Bell III, J.F., Gorelick, N., Hamilton, V.E., Ivanov, A., et al., 2003. Morphology and composition of the surface of Mars: Mars Odyssey THEMIS results. Science 300 (5628), 2056–2061. https://doi.org/10.1126/science.1080885.

Clark, B.C., Gellert, R., Ming, D.W., Morris, R.V., Mittlefehldt, D.W., Squyres, S.W., 2006. PYTi-NiCr Signatures in the Columbia Hills are present in certain Martian meteorites. In Lunar and Planetary Science Conference.

Clenet, H., Pinet, P., Ceuleneer, G., Daydou, Y., Heuripeau, F., Rosemberg, C., et al., 2013. A systematic mapping procedure based on the modified Gaussian model to characterize magmatic units from olivine/pyroxenes mixtures: application to the Syrtis Major volcanic shield on mars. J. Geophys. Res. Planets 118 (8), 1632–1655. https://doi.org/10.1002/jgre.20112.

Cousin, A., Sautter, V., Payré, V., Forni, O., Mangold, N., Gasnault, O., et al., 2017. Classification of igneous rocks analyzed by ChemCam at Gale crater, Mars. Icarus 288, 265–283. https://doi.org/10.1016/j.icarus.2017.01.014.

Day, J.M., Tait, K.T., Udry, A., Moynier, F., Liu, Y., Neal, C.R., 2018. Martian magmatism from plume metasomatized mantle. Nat. Commun. 9 (1), 4799. https://doi.org/10.1038/s41467-018-07191-0.

Demchuk, R.W., 2021. Detailed Mapping of Lava Flows in Syrtis Major Planum, Mars. Masters Thesis. Ohio University. http://rave.ohiolink.edu/etdc/view?acc_num=ohiou1617806602421614.

Dietrich, V.J., Gansser, A., Sommerauer, J., Cameron, W.E., 1981. Palaeogene komatiites from Gorgona island, East Pacific-A primary magma for ocean floor basalts? Geochem. J. 15 (3), 141–161. https://doi.org/10.2343/geochemj.15.141.

Duktig, B.R., 2023. Analyzing Compositional, Mineralogical, and Petrological Variations in Syrtis Major Planum Lava Flows throughout Martian Time. Masters Thesis. Ohio University. http://rave.ohiolink.edu/etdc/view?acc_num=ohiou1683243323834276.

Dunn, T.L., McSween Jr., H.Y., Christensen, P.R., 2007. Thermal emission spectra of terrestrial alkaline volcanic rocks: applications to Martian remote sensing. J. Geophys. Res. Planets 112 (E5). https://doi.org/10.1029/2006JE002766.

Dypvik, H., Hellevang, H., Krzesińska, A., Sætre, C., Viennet, J.C., Bultel, B., et al., 2021. The planetary terrestrial analogues library (PTAL)–an exclusive lithological selection of possible martian earth analogues. Planet. Space Sci. 208, 105339. https://doi.org/10.1016/j.pss.2021.105339.

Echeverria, L.M., 1980. Tertiary or Mesozoic komatiites from Gorgona island, Colombia: field relations and geochemistry. Contrib. Mineral. Petrol. 73 (3), 253–266. https://doi.org/10.1007/BF00381444.

Echeverría, L.M., Aitken, B.G., 1986. Pyroclastic rocks: another manifestation of ultramafic volcanism on Gorgona Island, Colombia. Contrib. Mineral. Petrol. 92 (4), 428–436. https://doi.org/10.1007/BF00374425.

Egger, M., Ebrahim, S., Smith, G.D., 2002. Where now for meta-analysis? Int. J. Epidemiol. 31 (1), 1–5. https://doi.org/10.1093/ije/31.1.1.

Ehlmann, B.L., Mustard, J.F., Murchie, S.L., Poulet, F., Bishop, J.L., Brown, A.J., et al., 2008. Orbital identification of carbonate-bearing rocks on mars. Science 322 (5909), 1828–1832. https://doi.org/10.1126/science.1164759.

Emran, A., Tarnas, J.D., Stack, K.M., 2025. Global distribution of serpentine on mars. Geophys. Res. Lett. 52 (2). https://doi.org/10.1029/2024GL110630 e2024GL110630.

Fawdon, P., 2016. The Volcanic Evolution of Syrtis Major Planum, Mars. Open University (United Kingdom).

Fawdon, P., Skok, J.R., Balme, M.R., Vye-Brown, C.L., Rothery, D.A., Jordan, C.J., 2015. The geological history of Nili Patera, Mars. J. Geophys. Res., Planets 120 (5), 951–977. https://doi.org/10.1002/2015JE004795.

Filiberto, J., 2017. Geochemistry of Martian basalts with constraints on magma genesis. Chem. Geol. 466, 1–14. https://doi.org/10.1016/j.chemgeo.2017.06.009.

Filiberto, J., 2019, July. Geochemistry of Martian Basalts: Support for Mars Sample Return of a Noachian/Hesperian Lava. In Ninth International Conference on Mars, vol. 2089, p. 6019.

Filiberto, J., Dasgupta, R., 2015. Constraints on the depth and thermal vigor of melting in the martian mantle. J. Geophys. Res. Planets 120 (1), 109–122. https://doi.org/10.1002/2014JE004745.
Filiberto, J., Gross, J., Trela, J., Ferré, E.C., 2014. Gabbroic shergottite northwest Africa 6963: an intrusive sample of mars. Am. Mineral. 99 (4), 601–606. https://doi.org/10.2138/am.2014.4638.
Gill, R., 2011. Igneous Rocks and Processes: A Practical Guide. Wiley-Blackwell. Chapter 5, p. 148, box 5.5.
Greenough, J.D., Ya'acoby, A., 2013. A comparative geochemical study of Mars and Earth basalt petrogenesis. Can. J. Earth Sci. 50 (1), 78–93. https://doi.org/10.1139/cjes-2012-0023.
Gross, J., Filiberto, J., Bell, A.S., 2013. Water in the martian interior: evidence for terrestrial MORB mantle-like volatile contents from hydroxyl-rich apatite in olivine–phyric shergottite NWA 6234. Earth Planet. Sci. Lett. 369, 120–128. https://doi.org/10.1016/j.epsl.2013.03.016.
Grove, T.L., Parman, S.W., 2004. Thermal evolution of the earth as recorded by komatiites. Earth Planet. Sci. Lett. 219 (3–4), 173–187. https://doi.org/10.1016/S0012-821X(04)00002-0.
Gurenko, A.A., Kamenetsky, V.S., Kerr, A.C., 2016. Oxygen isotopes and volatile contents of the Gorgona komatiites, Colombia: a confirmation of the deep mantle origin of H2O. Earth Planet. Sci. Lett. 454, 154–165. https://doi.org/10.1016/j.epsl.2016.08.035.
Hamilton, V.E., Christensen, P.R., 2000. Determining the modal mineralogy of mafic and ultramafic igneous rocks using thermal emission spectroscopy. J. Geophys. Res. Planets 105, 9717–9733. https://doi.org/10.1029/1999JE001113.
Hamilton, V.E., Wyatt, M.B., McSween Jr., H.Y., Christensen, P.R., 2001. Analysis of terrestrial and martian volcanic compositions using thermal emission spectroscopy: 2. application to martian surface spectra from the Mars Global Surveyor Thermal Emission Spectrometer. J. Geophys. Res. Planets 106 (E7), 14733–14746. https://doi.org/10.1029/2000JE001353.
Hamilton, V.E., Christensen, P.R., Mcsween, H.Y., Bandfield, J.L., 2003. Searching for the source regions of martian meteorites using MGS TES: integrating martian meteorites into the global distribution of igneous materials on mars. Meteorit. Planet. Sci. 38, 871–885. https://doi.org/10.1111/j.1945-5100.2003.tb00284.x.
Herzberg, C., Condie, K., Korenaga, J., 2010. Thermal history of the earth and its petrological expression. Earth Planet. Sci. Lett. 292 (1–2), 79–88. https://doi.org/10.1016/j.epsl.2010.01.022.
Hiesinger, H., Head III, J.W., 2004. The Syrtis Major volcanic province, Mars: synthesis from mars global surveyor data. J. Geophys. Res. Planets 109 (E1). https://doi.org/10.1029/2003JE002143.
Hood, D.R., Judice, T., Karunatillake, S., Rogers, D., Dohm, J.M., Susko, D., Carnes, L.K., 2016. Assessing the geologic evolution of Greater Thaumasia, Mars. J. Geophys. Res. Planets 121, 1753–1769. https://doi.org/10.1002/2016JE005046.
Hughes, E.B., Wray, J., Karunatillake, S., Fanson, G., Harrington, E., Hood, D.R., 2024. Water-limited hydrothermalism and volcanic resurfacing of Eridania Basin, Mars. J. Geophys. Res. 129 (7), e2024JE008461. https://doi.org/10.1029/2024JE008461.
ISO, 2014. SO 10788:2014(en) Space systems — Lunar simulants. Online Brows Platf. URL. https://www.iso.org/obp/ui#iso:std:iso:10788:ed-1:v1:en. accessed 05.20.25.
Jensen, L.S., Pyke, D.R., 1982. Komatiites in the Ontario Portion of the Abitibi Belt. Inist-CNRS & Bureau de Recherches Géologiques et Minières.
Kamenetsky, V.S., Gurenko, A.A., Kerr, A.C., 2010. Composition and temperature of komatiite melts from Gorgona Island, Colombia, constrained from olivine-hosted melt inclusions. Geology 38 (11), 1003–1006. https://doi.org/10.1130/G31143.1.
Kerr, A.C., 2005. La Isla de Gorgona, Colombia: a petrological enigma? Lithos 84 (1–2), 77–101. https://doi.org/10.1016/j.lithos.2005.02.006.
Kerr, A.C., Arndt, N.T., 2001. A note on the IUGS reclassification of the high-Mg and picritic volcanic rocks. J. Petrol. 42 (11), 2169–2171. https://doi.org/10.1093/petrology/42.11.2169.
Kerr, A.C., Marriner, G.F., Arndt, N.T., Tarney, J., Nivia, A., Saunders, A.D., Duncan, R. A., 1996a. The petrogenesis of Gorgona komatiites, picrites and basalts: new field, petrographic and geochemical constraints. Lithos 37 (2–3), 245–260. https://doi.org/10.1016/0024-4937(95)00039-9.
Kerr, A.C., Tarney, J., Marriner, G.F., Nivia, A., Klaver, G.T., Saunders, A.D., 1996b. The geochemistry and tectonic setting of late cretaceous Caribbean and Colombian volcanism. J. S. Am. Earth Sci. 9, 111–120. https://doi.org/10.1016/0895-9811(96)00031-4.
Koppers, A.A., Becker, T.W., Jackson, M.G., et al., 2021. Mantle plumes and their role in Earth processes. Nat. Rev. Earth Environ. 2 (6), 382–401. https://doi.org/10.1038/s43017-021-00168-6.
Le Maitre, R.W., Streckeisen, A., Zanettin, B., Le Bas, M.J., Bonin, B., Bateman, P. (Eds.), 2005. Igneous Rocks: A Classification and Glossary of Terms: Recommendations of the International Union of Geological Sciences Subcommission on the Systematics of Igneous Rocks. Cambridge University Press.
Lentz, R.F., Taylor, G.J., Treiman, A.H., 1999. Formation of a martian pyroxenite: A comparative study of the nakhlite meteorites and Theo's Flow. Meteorit. Planet. Sci. 34 (6), 919–932. https://doi.org/10.1111/j.1945-5100.1999.tb01410.x.
Lillis, R.J., Dufek, J., Kiefer, W.S., Black, B.A., Manga, M., Richardson, J.A., Bleacher, J. E., 2015. The Syrtis Major Volcano, Mars: A multidisciplinary approach to interpreting its magmatic evolution and structural development. J. Geophys. Res. Planets 120 (9), 1476–1496. https://doi.org/10.1002/2014JE004774.
Liu, Y., Tice, M.M., Schmidt, M.E., Treiman, A.H., Kizovski, T.V., Hurowitz, J.A., Allwood, A.C., Henneke, J., Pedersen, D.A.K., VanBommel, S.J., Jones, M.W.N., Knight, A.L., Orenstein, B.J., Clarck, B.C., Elam, W.T., Heirwegh, C.M., Barber, T., Beegle, L., Benzerara, K., Bernard, S., Beyssac, O., Bosak, T., Brown, A.J., Cardarelli, E.L., Catling, D.C., Christian, J.R., Cloutis, E.A., Cohen, B.A., Davidoff, S., Fairén, A.G., Farley, K.A., Flannery, D.T., Galvin, A., Grotzinger, J.P., Gupta, S., Hall, J., Herd, C.D.K., Hickman-Lewis, K., Hodyss, R.P., Horgan, B.H.N., Johnson, J. R., Jørgensen, J.L., Kah, L.C., Maki, J.N., Mandon, L., Mangold, N., McCubbin, F.M., McLennan, S.M., Moore, K., Nachon, M., Nemere, P., Nothdurft, L.D., Núñez, J.I., O'Neil, L., Quantin-Nataf, C.M., Sautter, V., Schuster, D.L., Siebach, K.L., Simon, J.I., Sinclair, K.P., Stack, K.M., Steele, A., Tarnas, J.D., Tosca, N.J., Uckert, K., Udry, R., Wade, L.A., Weiss, B.P., Wiens, R.C., Williford, K.H., Zorzano, M.P., 2022. An olivine cumulate outcrop on the floor of Jezero Crater. Mar. Sci. 377 (6614), 1513–1519. https://doi.org/10.1126/science.abo2756.
Lodders, K., 1998. A survey of shergottite, nakhlite and chassigny meteorites whole-rock compositions. Meteorit. Planet. Sci. 33 (S4), A183–A190. https://doi.org/10.1111/j.1945-5100.1998.tb01331.x.
Lunning, N.G., Gardner-Vandy, K.G., Sosa, E.S., McCoy, T.J., Bullock, E.S., Corrigan, C. M., 2017. Partial melting of oxidized planetesimals: an experimental study to test the formation of oligoclase-rich achondrites Graves Nunataks 06128 and 06129. Geochim. Cosmochim. Acta 214, 73–85. https://doi.org/10.1016/j.gca.2017.07.004.
Lustrino, M., Bonin, B., Doroshkevich, A., Kerr, Z.G.A., Heilborn, M., Irving, T., Ivanov, A., Mitchel, R., Nakawaga, M., Natland, J., Pearce, J., Scott-Smith, B., Srivastava, R., Tappe, S., Wilson, M., Zellmer, G., 2020. IUGS Task Group on Igneous Rocks TGIR.
McCollom, T.M., Seewald, J.S., 2013. Serpentinites, hydrogen, and life. Elements 9 (2), 129–134. https://doi.org/10.2113/gselements.9.2.129.
McGetchin, T.R., Smith, J.R., 1978. The mantle of mars: some possible geological implications of its high density. Icarus 34 (3), 512–536. https://doi.org/10.1016/0019-1035(78)90042-8.
McSween Jr., H.Y., 2015. Petrology on mars. Am. Mineral. 100 (11−12), 2380–2395. https://doi.org/10.2138/am-2015-5257.
McSween Jr., H.Y., Taylor, G.J., Wyatt, M.B., 2009. Elemental composition of the Martian crust. Science 324 (5928), 736–739. https://doi.org/10.1126/science.116587.
McSween, H.Y., McLennan, S.M., 2014. Mars. In: Holland, Heinrich D., Turekian, Karl K. (Eds.), Treatise on Geochemistry, Second edition, pp. 251–300. https://doi.org/10.1016/B978-0-08-095975-7.00125-X.
Mendes, L.N., Martinsson, O., Jamal, D.L., Zadeh, A.A., Wanhainen, C., 2025. Lithogeochemistry and origin of the komatiites from Mundonguara mine in the Manica Greenstone Belt, Mozambique. J. Afr. Earth Sci. 223, 105494. https://doi.org/10.1016/j.jafrearsci.2024.105494.
Metzger, P.T., Britt, D.T., Covey, S., Schultz, C., Cannon, K.M., Grossman, K.D., Mantovani, J., Mueller, R.P., 2019. Measuring the fidelity of asteroid regolith and cobble simulants. Icarus 321, 632–646. https://doi.org/10.1016/j.icarus.2018.12.019.
Meyer, C., 2012a. Los Angeles – 698 Grams Enriched Basaltic Shergottite. In: Martian Meteorite Compendium. NASA. https://curator.jsc.nasa.gov/antmet/mmc/. accessed 06.20.25.
Meyer, C., 2012b. Shergotty "Enriched" Basalt, 5 kg. In: Martian Meteorite Compendium. NASA. https://curator.jsc.nasa.gov/antmet/mmc/. accessed 06.20.25.
Meyer, C., 2012c. QUE94201 – 12.02 grams depleted basaltic shergottite. In: Martian Meteorite Compendium. NASA. https://curator.jsc.nasa.gov/antmet/mmc/. accessed 06.20.25.
Mikolajewicz, N., Komarova, S.V., 2019. Meta-analytic methodology for basic research: a practical guide. Front. Physiol. 10, 203. https://doi.org/10.3389/fphys.2019.00203.
Mustard, J.F., Erard, S., Bibring, J.P., Head, J.W., Hurtrez, S., Langevin, Y., Pieters, C.C: m, Sotin, C.J., 1993. The surface of syrtis major: composition of the volcanic substrate and mixing with altered dust and soil. J. Geophys. Res. Planets 98 (E2), 3387–3400. https://doi.org/10.1029/92JE02682.
Mustard, J.F., Murchie, S., Erard, S., Sunshine, J., 1997. In situ compositions of Martian Volcanics: implications for the mantle. J. Geophys. Res. Planets 102, 25605–25615. https://doi.org/10.1029/97JE02354.
Mustard, J.F., Poulet, F., Gendrin, A., Bibring, J.P., Langevin, Y., Gondet, B., Mangold, N., Bellucci, G., Altieri, F., 2005. Olivine and pyroxene diversity in the crust of mars. Science 307 (5715), 1594–1597. https://doi.org/10.1126/science.1109098.
Nair, A.M., Mathew, G., 2017. Geochemical modelling of terrestrial igneous rock compositions using laboratory thermal emission spectroscopy with an overview on its applications to Indian Mars Mission. Planet. Space Sci. 140, 62–73. https://doi.org/10.1016/j.pss.2017.04.009.
Nesbitt, R.W., Sun, S.S., Purvis, A.C., 1979. Komatiites; geochemistry and genesis. Can. Mineral. 17 (2), 165–186.
Ody, A., Poulet, F., Quantin, C., Bibring, J.-P., Bishop, J.L., Dyar, M.D., 2015. Candidates source regions of Martian meteorites as identified by OMEGA/MEx. Icarus 258, 366–383. https://doi.org/10.1016/j.icarus.2015.05.019.
Pearce, J.A., 2008. Geochemical fingerprinting of oceanic basalts with applications to ophiolite classification and the search for Archean oceanic crust. Lithos 100 (1–4), 14–48. https://doi.org/10.1016/j.lithos.2007.06.016.
Peters, G.H., Abbey, W., Bearman, G.H., Mungas, G.S., Smith, J.A., Anderson, R.C., Douglas, S., Beegle, L.W., 2008. Mojave mars simulant—characterization of a new geologic mars analog. Icarus 197, 470–479. https://doi.org/10.1016/j.icarus.2008.05.004.
Poulet, F., Mangold, N., Platevoet, B., Bardintzeff, J.-M., Sautter, V., Mustard, J.F., Bibring, J.-P., Pinet, P., Langevin, Y., Gondet, B., Aléon-Toppani, A., 2009. Quantitative compositional analysis of Martian mafic regions using the MEx/OMEGA reflectance data. Icarus 201, 84–101. https://doi.org/10.1016/j.icarus.2008.12.042.
Putirka, K., 2016. Rates and styles of planetary cooling on Earth, Moon, Mars, and Vesta, using new models for oxygen fugacity, ferric-ferrous ratios, olivine-liquid Fe-Mg

exchange, and mantle potential temperature. Am. Mineral. 101 (4), 819–840. https://doi.org/10.2138/am-2016-5402.
R Core Team, 2024. R: A Language and Environment for Statistical Computing. R Foundation for Statistical Computing, Vienna, Austria. https://www.R-project.org/&gt.
Ramkissoon, N.K., Pearson, V.K., Schwenzer, S.P., Schröder, C., Kirnbauer, T., Wood, D., et al., 2019. New simulants for Martian regolith: controlling iron variability. Planet. Space Sci. 179, 104722. https://doi.org/10.1016/j.pss.2019.104722.
Rampey, M., Harvey, R., 2012. Mars Hesperian magmatism as revealed by Syrtis major and the Circum-Hellas volcanic province. Earth Moon Planet. 109, 61–75. https://doi.org/10.1007/s11038-012-9404-0.
Ramsey, M.S., Christensen, P.R., 1998. Mineral abundance determination: Quantitative deconvolution of thermal emission spectra. J. Geophys. Res. Solid Earth 103, 577–596. https://doi.org/10.1029/97JB02784.
Rani, A., Basu Sarbadhikari, A., Hood, D.R., Gasnault, O., Nambiar, S., Karunatillake, S., 2022. Consolidated chemical provinces on mars: implications for geologic interpretations. Geophys. Res. Lett. 49 (14). https://doi.org/10.1029/2022GL099235 e2022GL099235.
Ray, D., Misra, S., 2015. Martian basalts-planetary analogue of terrestrial MORBs?. In: European Planetary Science Congress. Europlanet, Nantes, France, p. 47.
Révillon, S., Arndt, N.T., Chauvel, C., Hallot, E., 2000. Geochemical study of ultramafic volcanic and plutonic rocks from Gorgona island, Colombia: the plumbing system of an oceanic plateau. J. Petrol. 41 (7), 1127–1153. https://doi.org/10.1093/petrology/41.7.1127.
Révillon, S., Chauvel, C., Arndt, N.T., Pik, R., Martineau, F., Fourcade, S., Marty, B., 2002. Heterogeneity of the Caribbean plateau mantle source: Sr, o and he isotopic compositions of olivine and clinopyroxene from Gorgona island. Earth Planet. Sci. Lett. 205 (1–2), 91–106. https://doi.org/10.1016/S0012-821X(02)01003-8.
Reyes, D.P., Christensen, P.R., 1994. Evidence for komatiite-type lavas on mars from Phobos ISM data and other observations. Geophys. Res. Lett. 21 (10), 887–890. https://doi.org/10.1029/94GL01002.
Richards, M.A., Duncan, R.A., Courtillot, V.E., 1989. Flood basalts and hot-spot tracks: plume heads and tails. Science 246 (4926), 103–107. https://doi.org/10.1126/science.246.4926.103.
Rickman, D., Hoelzer, H., Carpenter, P., Sibille, L., Howard, R., Owens, C., 2007. A quantitative method for evaluating regolith simulants. In: AIP Conference Proceedings, vol. 880. American Institute of Physics, pp. 957–963. https://doi.org/10.1063/1.2437539. No. 1.
Rickman, D., Hoelzer, H., Fourroux, K., 2009. Lunar Regolith Figures of Merit. In Lunar Regolith/Simulant Workshop (No. MSFC-2219).
Riel, N., Duarte, J.C., Almeida, J., Kaus, B.J., Rosas, F., Rojas-Agramonte, Y., Popov, A., 2023. Subduction initiation triggered the Caribbean large igneous province. Nat. Commun. 14 (1), 786. https://doi.org/10.1038/s41467-023-36419-x.
Rubin, A.E., Warren, P.H., Greenwood, J.P., Verish, R.S., Leshin, L.A., Hervig, R.L., et al., 2000. Los Angeles: the most differentiated basaltic Martian meteorite. Geology 28 (11), 1011–1014. https://doi.org/10.1130/0091-7613(2000)28<1011:LATMDB>2.0.CO;2.
Salvatore, M.R., Mustard, J.F., Wyatt, M.B., Murchie, S.L., 2010. Definitive evidence of Hesperian basalt in Acidalia and Chryse planitiae. J. Geophys. Res. 115, E07005. https://doi.org/10.1029/2009JE003519.
Salvatore, M.R., Goudge, T.A., Bramble, M.S., Edwards, C.S., Bandfield, J.L., Amador, E. S., et al., 2018. Bulk mineralogy of the NE Syrtis and Jezero crater regions of mars derived through thermal infrared spectral analyses. Icarus 301, 76–96. https://doi.org/10.1016/j.icarus.2017.09.019.
San Martin, J., Leone, G., Riveros-Jensen, K., Alam, M.A., Cabrera, R., San Martin, D., Oses, R., Blamey, J., Demergasso, C., Abrevaya, X., Guiliani, N., Britt, D., Liu, Y., Silva, W., Slumba, K., Tovar, D., Leal, M.A., de Pablo, M.A., 2025. Prospecting the first Chilean Martian simulants from the Atacama Desert for ISRU and potential applications. Icarus 429, 116403. https://doi.org/10.1016/j.icarus.2024.116403.
Scott, A.N., Oze, C., Tang, Y., O'Loughlin, A., 2017. Development of a Martian regolith simulant for in-situ resource utilization testing. Acta Astronaut. 131, 45–49. https://doi.org/10.1016/j.actaastro.2016.11.024.
Serrano, L., Ferrari, L., Martínez, M.L., Petrone, C.M., Jaramillo, C., 2011. An integrative geologic, geochronologic and geochemical study of Gorgona Island, Colombia: implications for the formation of the Caribbean Large Igneous Province. Earth Planet. Sci. Lett. 309 (3–4), 324–336. https://doi.org/10.1016/j.epsl.2011.07.011.
Shimizu, K., Shimizu, N., Komiya, T., Suzuki, K., Maruyama, S., Tatsumi, Y., 2009. CO2-rich komatiitic melt inclusions in Cr-spinels within beach sand from Gorgona Island, Colombia. Earth Planet. Sci. Lett. 288 (1–2), 33–43. https://doi.org/10.1016/j.epsl.2009.09.005.
Sibille, L., Carpenter, P., Schlagheck, R., French, R.A., 2006. Lunar Regolith Simulant Materials: Recommendations for Standardization, production, and usage (No. NASA/TP-2006-214605). NASA Technical Publication.
Stolper, E., McSween Jr., H.Y., 1979. Petrology and origin of the shergottite meteorites. Geochim. Cosmochim. Acta 43 (9), 1475–1498. https://doi.org/10.1016/0016-7037(79)90142-X.
Storey, M., Mahoney, J.J., Kroenke, L.W., Saunders, A.D., 1991. Are oceanic plateaus sites of komatiite formation? Geology 19 (4), 376–379. https://doi.org/10.1130/0091-7613(1991)019<0376:AOPSOK>2.3.CO;2.
Sutton, A.J., Higgins, J.P., 2008. Recent developments in meta-analysis. Stat. Med. 27 (5), 625–650. https://doi.org/10.1002/sim.2934.
Taylor, G.J., 2009. Ancient lunar crust: origin, composition, and implications. Elements 5 (1), 17–22. https://doi.org/10.2113/gselements.5.1.17.
Taylor, G.J., Martel, L.M.V., Karunatillake, S., Gasnault, O., Boynton, W.V., 2010. Mapping mars geochemically. Geology 38, 183–186. https://doi.org/10.1130/G30470.1.
Tosca, N.J., Tice, M.M., Hurowitz, J.A., Pedersen, D.A., Henneke, J., Mandon, L., et al., 2025. In situ evidence for serpentinization within the Máaz Formation, Jezero Crater, Mars. Sci. Adv. 11 (27), eadr8793. https://doi.org/10.1126/sciadv.adr8793.
Treiman, A.H., 2003. Chemical compositions of Martian basalts (shergottites): some inferences on b; formation, mantle metasomatism, and differentiation in mars. Meteorit. Planet. Sci. 38 (12), 1849–1864.
Trikalinos, T.A., Salanti, G., Zintzaras, E., Ioannidis, J.P., 2008. Meta-analysis methods. Adv. Genet. 60, 311–334. https://doi.org/10.1016/S0065-2660(07)00413-0.
Verma, S.K., Oliveira, E.P., Silva, P.M., Moreno, J.A., Amaral, W.S., 2017. Geochemistry of komatiites and basalts from the Rio das Velhas and Pitangui greenstone belts, São Francisco craton, Brazil: implications for the origin, evolution, and tectonic setting. Lithos 284, 560–577. https://doi.org/10.1016/j.lithos.2017.04.024.
Vickery, A.M., Melosh, H.J., 1987. The large crater origin of SNC meteorites. Science 237, 738–743. https://doi.org/10.1126/science.237.4816.738.
Waterton, P., Arndt, N., 2023. Komatiites: their geochemistry and origins. In: The Archaean Earth: Tempos and Events (2nd Edition of The Precambrian 12Earth). Elsevier. https://doi.org/10.31223/X5PX0X.
Werner, S.C., Ody, A., Poulet, F., 2014. The source crater of Martian shergottite meteorites. Science 343, 1343–1346. https://doi.org/10.1126/science.1247282.
Wyatt, M.B., Hamilton, V.E., McSween, H.Y., Christensen, P.R., Taylor, L.A., 2001. Analysis of terrestrial and Martian volcanic compositions using thermal emission spectroscopy: 1. Determination of mineralogy, chemistry, and classification strategies. J. Geophys. Res. Planets 106, 14711–14732. https://doi.org/10.1029/2000JE001356.
Wyatt, M.B., McSween, H.Y., 2007, May. TES and GRS compositions of the Martian surface: evidence for igneous and secondary chemical fractionation processes. In: AGU Spring Meeting Abstracts, vol. 2007 pp. P31A-07.
Zalewska, N.E., Mroczkowska-Szerszeń, M., Fritz, J., Błęcka, M., 2018. Modeling of surface spectra with and without dust from Martian infrared data: new aspects. Aircr. Eng. Aerosp. Technol. 91 (2), 333–345. https://doi.org/10.1108/AEAT-01-2018-0051.